IDA | RESEARCH NOTES

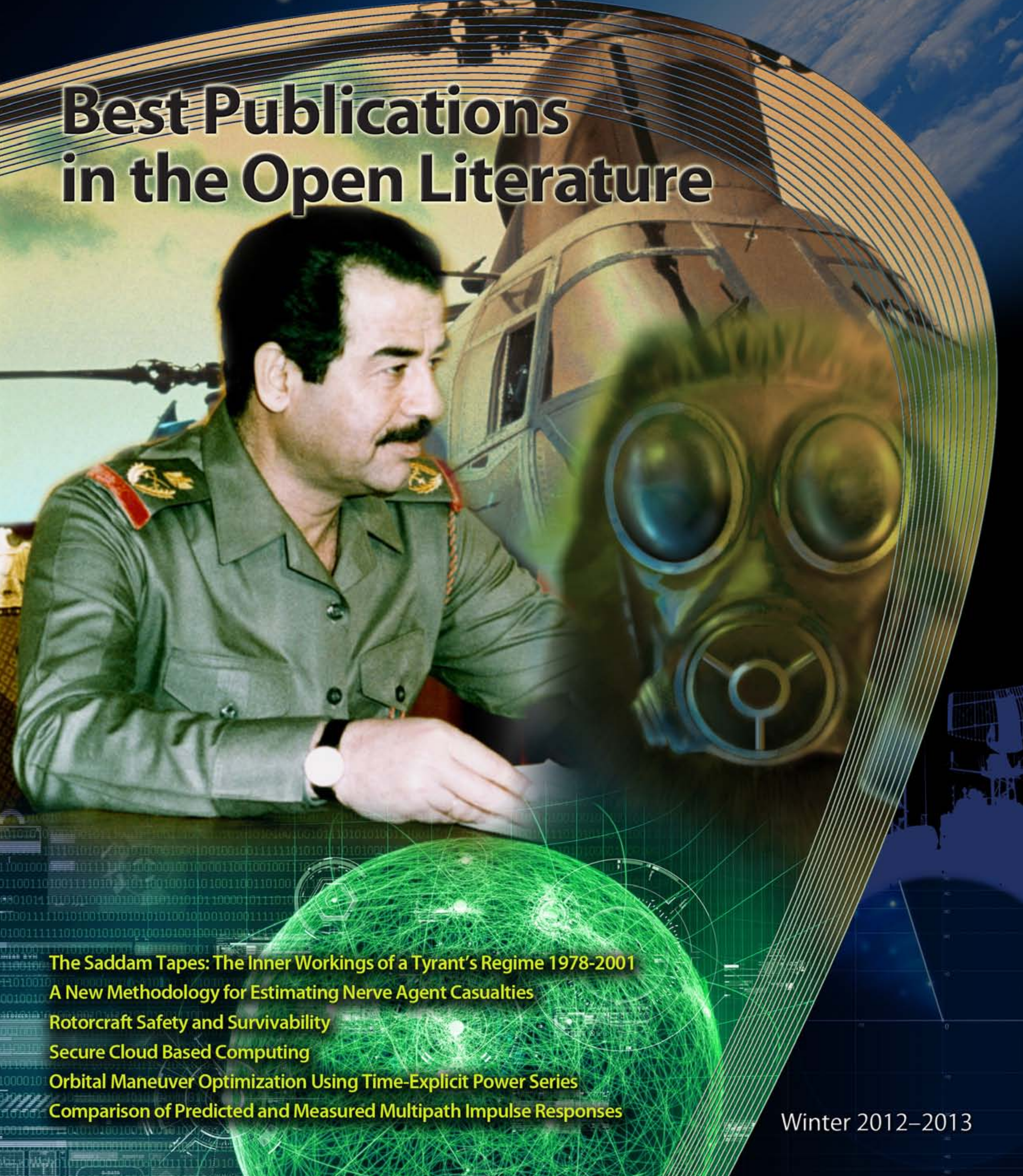

Best Publications in the Open Literature

The Saddam Tapes: The Inner Workings of a Tyrant's Regime 1978-2001
A New Methodology for Estimating Nerve Agent Casualties
Rotorcraft Safety and Survivability
Secure Cloud Based Computing
Orbital Maneuver Optimization Using Time-Explicit Power Series
Comparison of Predicted and Measured Multipath Impulse Responses

Winter 2012–2013

Dr. Kevin Woods (center) is presented the Larry D. Welch Award for Best External Publication from Gen. Larry D. Welch, (Ret.) (left), Senior Fellow, Institute for Defense Analyses and Dr. David S.C. Chu, President, Institute for Defense Analyses.

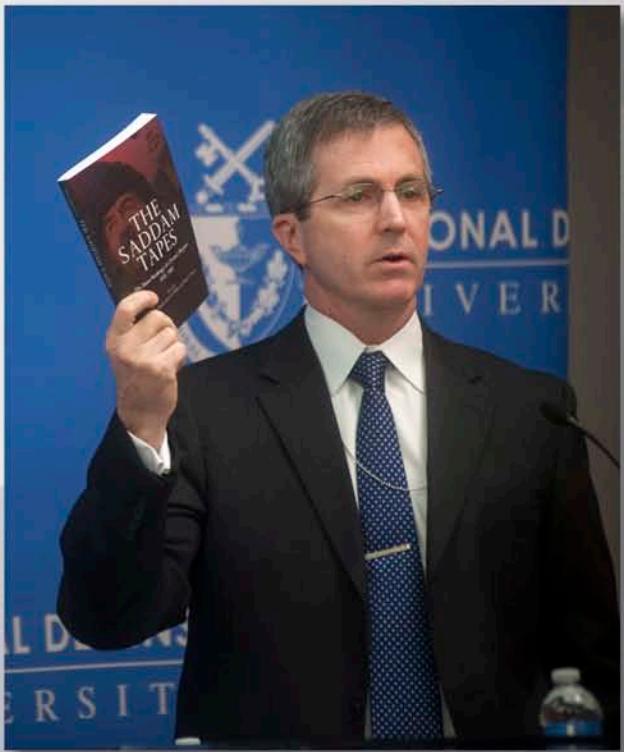

Dr. Kevin Woods delivers a presentation to members of the Department of Defense, State Department, congressional staffs and academia on the book he co-edited *The Saddam Tapes: The Inner Workings of a Tyrant's Regime 1978-2001* at the National Defense University. During the discussion, Dr. Woods outlined the history behind the book and gave examples of what the book reveals about the late Iraqi dictator.

IDA is the Institute for Defense Analyses, a non-profit corporation operating in the public interest.

IDA's three federally funded research and development centers provide objective analyses of national security issues and related national challenges, particularly those requiring extraordinary scientific and technical expertise.

IDA | THE WELCH AWARD

This issue of IDA Research Notes is dedicated to the winner and finalists of IDA's inaugural Larry D. Welch Award for best external publication. Named in honor of former IDA president and US Air Force Chief of Staff, General Larry Welch, the award recognizes individuals who exemplify General Welch's high standards of analytic excellence through their publication in peer-reviewed journals or other professional publications, including books and monographs. The articles in this edition are executive summaries of the original published pieces. We have identified and credited the original publication for each article and, where possible, we have included a link or Quick Response (QR) code to the full piece.

Winner

IDA researcher **Kevin Woods**, and his co-editors, **David Palkki** and **Mark Stout**, culled through thousands of hours of Saddam's private recordings to provide a unique look into the Iraqi regime. *The Saddam Tapes: The Inner Workings of a Tyrant's Regime 1978-2001*, published by Cambridge University Press, includes annotated transcripts of audio-taped conversations between Saddam Hussein and his inner circle.

Finalist

The research team of **Deena Disraelly**, **Terri Walsh**, **Robert Zirkle**, and **Carl Curling** describes a methodology created for estimating casualties resulting from exposure to the nerve agent Sarin in "A New Methodology for Estimating Nerve Agent (Sarin (GB)/VX) Casualties as a Function of Time: Defining the Human Response Injury Profile Nerve Agent Methodology." The full paper was published in the September–October 2011 edition of the *Journal of Chemical Health and Safety*.

Finalist

Mark Couch and his co-author Dennis Lindell, studied rotorcraft losses during Operations Enduring and Iraqi Freedom. Their analysis, "Rotorcraft Safety and Survivability," was published in the *Proceedings of the 66th American Helicopter International Annual Forum 2010*. They conclude that the US military has reduced rotorcraft loss rates since Vietnam but that more can be done.

Finalist

Coimbatore Chandersekaran, William Simpson, and **Ryan Wagner** describe how the Department of Defense can take advantage of cloud computing while meeting its integrity and security requirements. "High Assurance Challenges for Cloud Based Computing" was published in the *Proceedings of the World Congress on Engineering and Computer Science 2011*.

Finalist

James Thorne's article, "Orbital Maneuver Optimization Using Time-Explicit Power Series," published in the journal *Celestial Mechanics and Dynamical Astronomy*, presents an analytical method for optimizing orbital maneuvers that minimizes the fuel use.

Finalist

Examining the issue of predicting multipath radar responses, **Kent Haspert** and **Michael Tuley** present a slightly modified version of the original analytical approaches for evaluating multipath effects in the article "Comparison of Predicted and Measured Multipath Impulse Responses," published in the journal *IEEE Transactions on Aerospace and Electronic Systems*.

THE SADDAM TAPES: THE INNER WORKINGS OF A TYRANT'S REGIME 1978-2001

Kevin Woods

Winner

Why do you think we trusted the Prophets? It is because they recorded every incident.

—Saddam Hussein, circa 1987

Following the rapid collapse of the Ba'ath regime in 2003, the US government captured an extensive collection of media files and documents, including audio recordings of Saddam Hussein exercising power behind closed doors. An IDA-led team spent 5 years culling through summary transcripts and audio files from the collection, selecting those in which Saddam was a key participant in discussions revolving around Iraqi national security or international relations.

The following article summarizes the resulting information compiled in *The Saddam Tapes: The Inner Workings of a Tyrant's Regime 1978-2001,* which reveals the former Iraqi leader as a capable, intelligent, but undisciplined decision maker. He was anti-Semitic, held grandiose notions of Iraq leading the Arab world, was overly sanguine about Iraq's ability to prevail in war against its enemies, was cautious about using chemical weapons, and thought the United States was determined to destroy his regime. The value of this kind of historical research extends well beyond documenting the history of one dictator. The captured records on which this work is based offer lessons and insights into critical contemporary issues such as the proliferation of weapons of mass destruction, deterrence, international sanctions, state relationships with non-state actors, and the methods of totalitarian state control.

Saddam expressed a strong belief that the United States was engaged in a conspiracy to contain and destroy his regime.

Fortunately for history, Saddam meticulously recorded private office conversations. In this way he could manage his legacy and track the huge volume of decisions necessary to maintain an iron grip on power. The several thousand hours of audio and video recordings reviewed in the development of *The Saddam Tapes* illuminate many of the regime's decisions, decision-making processes, perspectives, and personalities.

The model for *The Saddam Tapes* and related research was a series of similar efforts in the decades after World War II. The most notable among them are the US Army's use of the German perspective in its official histories ("Green Books") of the war, the chilling documents revealed in the Nuremberg War Crimes Tribunals, the publication of the Department of State's Nazi-Soviet Relations 1939–1941 collection of documents, and the work of Harvard University's Russian Research Center, where, in 1958, Merle Fainsod produced his seminal work, *Smolensk* *under Soviet Rule*. IDA's basic research approach required creating an archival collection out of what is an intelligence repository. The editors led a team that reviewed summary transcripts of more than 7,000 audio files to categorize and reduce the collection size. This review allowed the identification and translation of 900 tapes on which Saddam was central to the dialogue and the focus was on Iraqi national security or international relations. The subtopics addressed in this smaller collection were further refined and sorted into roughly eight chapters described below. Another editorial board using the same criteria would certainly have chosen different tapes or selections. In an effort to maximize the potential value of the captured records at the heart of this research, IDA's Joint Advanced Warfighting Division designed and brought to life the Conflict Records Research Center (CRRC) at National Defense University. Sponsored by the Office of the Under Secretary of Defense for Policy, the CRRC makes available to the scholarly community digital copies of the transcripts of conversations presented here, as well as digital copies of tens of thousands of pages of other Iraqi state records and al-Qaeda-related documents.

United States Against Iraq

The first chapter deals with Saddam's views of the United States. His private view of the country, its policies, and enduring interests was generally consistent during the period covered. Saddam expressed a strong belief that the United States was engaged in a generation-long conspiracy to contain and destroy his regime. This wide-ranging conspiracy, while not without the

Saddam and former Vice President of Iraq Taha Ramadan share a laugh (date unknown). **Credit**: Conflict Records Research Center.

occasional confirmatory evidence such as the Iran-Contra scandal, remained the framework within which all interactions were considered. Interest did not translate into understanding however. In one conversation, Saddam noted that he found America a "complicated country" with a "confusing" political process. Despite this gap, Saddam reserved for himself the role of Iraq's senior American political and strategic analyst. Emphasizing that political analysis was not the domain of intelligence services, Saddam went on to declare that his "basis of analysis" would be that which he used when judging Iran "… some of it out of deduction and some of it through intuition … making connections between issues without having hard evidence." One should not be surprised that he professed to believe that the outcome of the 1992 US presidential election was proof he prevailed in the 1991 Gulf War. Bush, Saddam concluded "… put himself in the position that it's either him or Iraq … Bush fell and Iraq lasted."

Intense Anti-Semitism

Chapter two examines Saddam's views toward Israel or "the Zionist Enemy," as Iraq's senior leadership most commonly referred to it. While the tapes make clear that Saddam was, at times, consumed by concern about Israel's military superiority, they also leave no doubt that his anti-Semitism was deep and abiding. Otherwise serious policy discussions were often supported by references to anti-Semitic propaganda like *The Protocols of the Elders of Zion*. At other times, however, Saddam expressed a degree of admiration for his "unusually smart" adversary whose audacity, including the ability to "direct" the Iranians during the Iran-Iraq War or to act as the real conspirator behind the 1993 World Trade Center bombing, was such that "the Arab mentality" had a hard time grasping it.

Head of the Arab World

The third chapter describes Saddam's often fitful relationship with the other states and actors in the Arab world. A near constant theme in Saddam's regional political maneuverings was his belief in Iraq's historical destiny to lead the Arab world—not an easy task given regional rivalries, Saddam's invasion of a fellow Arab state, and his proclivity to meddle openly in the politics of neighboring states. Saddam's distrust of many of his fellow Arab leaders ran from derision, in the case of "those who work politics under the guise of religion" to disgust, describing them variously as "Arabs of decay [and] shame," "actors … liars" and "conspirators." In a chilling reflection of characters in *The Godfather* movies or the HBO television series *The Sopranos*, Saddam's regional diplomatic style ran the gamut from homicidal to familial. Discussions with his senior advisors included how to foster revolts or, in some cases, assassinate uncooperative regional leaders. For example, in 1978, during a particularly fractious period in the history of the Palestinian Liberation Organization, Saddam declared that its leader, Yasser Arafat, was "… not the true representative of the Palestinian revolution [so] … let one of the brave Iraqis among the crowd draw his pistol and shoot [him] … [because] behind that headband of Arafat there is an evil brain." A decade later, Arafat was in Baghdad to pledge support for Iraq on the eve of Operation Desert Storm. After discussing possible terrorist counters to an American attack, Saddam thanked Arafat for his efforts and assured him that "you are either an enemy or a friend … you can't have something in the middle."

Long War

Chapter four samples the many tapes recorded during the 1980–1988 Iran-Iraq War. This inconclusive struggle has the distinction of being one of the largest, deadliest, and yet least documented wars of the twentieth century. Unlike many conflicts in the closing decades of the last century, the Iran-Iraq War featured many of the worst aspects of warfare from the early decades: endless trenches, mindless frontal assaults, and chemical weapons. The tape selections provide glimpses into the overly optimistic military assessments and naive political calculations that convince Saddam he could, in a few short weeks, "… stick their noses in mud so we can impose our political will over them." The realization of a long war led Saddam and his advisors to discuss horrific means to bring it to an end, including a proposal to "… mount a heavy chemical strike equivalent to an atomic weapon and totally annihilate that city so that no living soul will survive." This chapter reveals a regime beset by battlefield and international struggles and challenged by shifting alliances and military fortunes. However, it also shows a dictator capable of learning—at the cost of over a million casualties.

Kuwait Attack

The fifth chapter covers Iraq's disastrous 1990 invasion and occupation of Kuwait and the subsequent "Mother of all Battles" that eventually drove Iraq out. In a repeat of many of the mistakes of the Iran-Iraq War, the tapes reveal a stunning lack of planning, foresight, or consensus, not only on the invasion but also on basic questions of what Iraq should do with its newest province. Saddam asked his ministers a few days after the operation began "what is the future of the Iraqi-Kuwaiti relation now? … We need to get going … every day that goes by, we don't know what the next day is going to bring us!" Saddam is seen as an active and engaged leader throughout this period. For example, in addition to suggesting improvements to the efforts to denude Kuwait of its material wealth, Saddam approved the murder of Kuwaiti civilians, helped to plan the destruction of Kuwait's oil fields, authorized the release of crude oil and free-floating mines into the Gulf, directed the timing and priority of Scud missile targets in Israel and Saudi Arabia, and made the final decision to withdraw from Kuwait by noting it was better than "… letting the enemy doing it for you!" It is clear from this material that Saddam never appreciated his strategic or military position. In one tape, he offers a bit of classic self-serving analysis, which, it might be argued, played a part in his ultimate demise. Looking back at the war a year after it ended, Saddam mused, "let's suppose that their military won …

Saddam and senior advisors (Nov. 2002). **Credit**: Conflict Records Research Center.

[the coalition has the] strongest scientific, technological, and military powers and highest financial and economic potential existing in the region and the world without any exception. They all got together against us, and they did not succeed despite what happened. They did not dare attack Baghdad. They did not dare launch [an] attack on Baghdad [even] after 6 months elapsed … . Such a condition has never happened in all the wars of the world." Victory is in the eye of the beholder.

Chemical Weapons

The final three chapters cover, respectively, the related subjects of weapons of mass destruction (WMD), international sanctions, and the strange tale of Saddam's son-in-law. While many of these subjects were in all likelihood considered too sensitive for even Saddam's private recording system, the tapes provide a glimpse into the mindsets, assumptions, and complex motivations associated with WMD. For example, Saddam recognized early in the Iran-Iraq War that "… sometimes what you get out of a weapon is when you keep saying, I will bomb you, [and] it is actually better than bombing him. It is possible that when you bomb him, the material effect will be 40 percent, but, if you stick it up to his face, the material and the spiritual effect will be

60 percent, so why hit him? Keep getting 60 percent!" This perhaps explains his occasional caution in disapproving proposals to use chemical weapons. In a discussion about targeting a Kurdish group, Saddam opined that "I believe that we, as a command, we should be prepared to use even the special arsenal if there is a target worth doing that. It would be better, of course, to resort to conventional weapons." Saddam's early guidance on United Nations' and other inspection teams set the tone for the 1990s with "we should not go to war because of [inspections] … but at least let us harass our enemy. We should not harass them with our refusal, not harass them with our acceptance, but we should always place lines for them to cross, lines between refusal and acceptance … ." Finally, the last chapter briefly highlights one of the strangest episodes in Saddam's colorful life: the defection, forgiveness, and subsequent murder of the head of Iraq's WMD programs and Saddam's own son-in-law, Hussein Kamil. While the outcome of this episode seemed foreordained, the mix of family and state betrayal that led the dictator to declare of a close family member that "… he is horrible, and we need to get rid of him" adds a degree of family drama to otherwise cold discussions on proliferation.

Conclusion

Overall, Saddam emerges from this manuscript as a highly competent, intelligent, but intellectually undisciplined decision maker—a lively, quick-witted, and fickle man given to restless digressions on a surprising range of topics, many of which he appeared to understand poorly or in decidedly unique ways. He was also brutal, deceptive, arrogant, and grandiose. At times, his worldview, borrowing a British diplomat's description of Stalin, consisted of a "curious mix of shrewdness and nonsense" (Andrew and Elkner 2003, 77). These are important historical lessons worth reinforcing and updating from time to time. Totalitarian regimes provide few opportunities to develop understanding of their leaders. *The Saddam Tapes* will not solve the lack of access to the decision-making process of some future tyrant, but it can improve analysts' ability to appreciate unfamiliar decision-making processes and the limits of their own judgments about the other side's intent. Ironically, one of the most opaque regimes of the late twentieth century may, because of these tapes, become one of the most transparent.

Dr. Woods is a research staff member and historian in IDA's Joint Advanced Warfighting Division. He earned his doctorate in history from the University of Leeds, UK.

The Saddam Tapes: The Inner Workings of a Tyrant's Regime 1978-2001, published in 2011 by Cambridge University Press.

BEHIND-THE-SCENES LOOK AT IRAQI REGIME HONORED WITH WELCH AWARD

http://vimeo.com/33188406

REFERENCES

All quotations from Iraqi records are drawn from Woods, Kevin M., David D. Palkki, and Mark Stout, eds. 2011. *The Saddam Tapes: The Inner Workings of a Tyrant's Regime 1978-2001.* New York: Cambridge University Press.

Andrew, Christopher, and Julie Elkner. 2003. "Stalin and Foreign Intelligence." *Totalitarian Movements and Political Religions* 4 (1) (Summer): 69–94.

A NEW METHODOLOGY FOR ESTIMATING NERVE AGENT CASUALTIES

Deena S. Disraelly, Terri J. Walsh, Robert A. Zirkle, and Carl A. Curling

The Human Response Injury Profile (HRIP) methodology was developed to provide planners an improved ability to estimate casualties resulting from exposure to chemical, biological, radiological, and nuclear (CBRN) agents or effects. The methodology relies on time-based progressions of underlying symptoms and their severity changes to determine user-defined casualty estimates following CBRN events.

The HRIP methodology provides the capability to estimate the time-dependence of the numbers of individuals wounded and killed, a procedure that aids in the development of medical and logistics requirements, acquisition, and planning. The methodology also characterizes the incidence of injury by severity to provide additional information to assist planners. Further, the HRIP methodology allows the user to define the casualty threshold—the severity at which casualties occur. This capability means that the user can determine the patient loads and how these loads might change as a function of injury (and symptom) severity.

The following article summarizes "A New Methodology for Estimating Nerve Agent (Sarin (GB)/VX) Casualties as a Function of Time," an article that appeared in the September–October 2011 issue of the *Journal of Chemical Health and Safety* and was paired with a companion piece, "Defining the Human Response Injury Profile Methodology." The overall purpose of the pair of articles was to describe one application of the HRIP methodology: the HRIP nerve agent methodology used to estimate casualties resulting from exposure to nerve agents Sarin (GB) and VX.

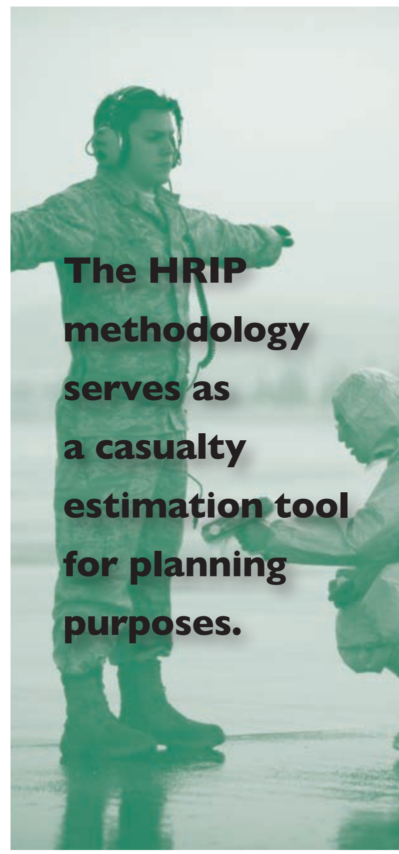

In the first article, the authors described the development of the HRIP nerve agent methodology. The article summarized here expands on the HRIP nerve agent methodology, describing how the methodology can be employed to estimate casualties and fatalities over time. These articles are part of a larger series of articles published (or currently in draft) that describe the HRIP methodology as it applies to other types of weapons of mass destruction, including chemical mustard, contagious and noncontagious biological agents, radiological hazards, and nuclear detonations.

HRIP NERVE AGENT METHODOLOGY IMPLEMENTATION

The HRIP nerve agent methodology is built upon three precepts: that the severity of symptoms can be expressed on a single uniform scale, regardless of the cause of the symptoms; that an injury resulting from nerve agent exposure can be described by a progression of symptoms over time (known as an injury profile); and that the casualty status of an injured individual can be directly related to the severity of symptoms manifest at any specified time. The fundamental concept of the HRIP methodology builds on these precepts to state that an individual is considered a casualty at the time of first onset of injury-specific symptoms at or above a user-specified severity (or casualty) threshold.

In general, the HRIP methodology entails a series of injury profiles (one for each HRIP-defined dose/dosage band), which are graphical depictions of symptom progression over time on a severity scale ranging from 0 (no effect) to 4 (very severe). The HRIP nerve agent methodology consists of either one or two sets of injury profiles, for GB and VX respectively: one set of injury profiles for vapor inhalation (GB and VX), and a second set of injury profiles for liquid percutaneous exposures (VX only). Any scenario describing a nerve agent attack will include a collection of individuals, each of whom will receive an inhalation dosage and (for VX) a percutaneous dose, which are then input to the methodology.[1] An additional input is the time the nerve agent exposure ends relative to some starting time (t_0 typically taken as the time of the agent release). Given these inputs, the HRIP nerve agent methodology can be used to estimate the casualty status of individuals. The methodology produces as output an aggregate casualty status over time for all individuals contained in the scenario. The HRIP methodology itself consists of two components, as shown in Figure 1: "Human Response Estimation" and "Casualty Estimation and Reporting." Each component will be described below.

Human Response Estimation Component

The first component of the HRIP nerve agent methodology, the human response estimation component, is used to estimate the response of individuals to a combination of vapor

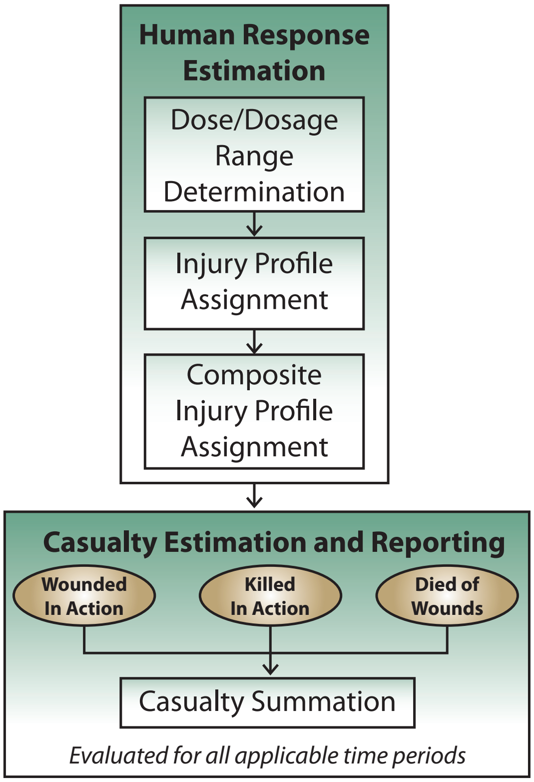

Figure 1. HRIP Methodology for Nerve Agents
Credit: *Journal of Chemical Health and Safety* 18 (5) (2010).

[1] The exposure estimations are derived external to the HRIP methodology, employing a user-selected tool or model to estimate chemical agent cloud concentrations and depositions, which are then combined with scenario-relevant warning and protection factors to estimate exposures.

inhalation dosages and percutaneous liquid doses in terms of the type and severity of injury over time (i.e., the injury profile). This calculation entails a three-step process: determination of inhalation dosage and percutaneous dose ranges; assignment of injury profiles based upon those ranges; and combining those injury profiles into a single composite injury profile, as required. For nerve agents, the composite injury profile is used to determine if and when individuals become casualties and fatalities.

Casualty Estimation and Reporting Component

For the HRIP nerve agent methodology, a chemical casualty is defined as any person who is lost to his organization by reason of having been declared dead or wounded as a result of exposure to a chemical agent (NATO 2002, 10). The HRIP nerve agent methodology estimates three classes of casualty: individuals killed in action (KIA), individuals wounded in action (WIA), and individuals who died of wounds (DOW).

A KIA is defined as "a battle casualty who is killed outright or who dies as a result of wounds or other injuries before reaching a medical treatment facility [MTF]" (NATO 2010, 2-K-1). A WIA is "a battle casualty other than 'killed in action' who has incurred an injury due to an external agent or cause" (NATO 2010, 2-W-2) and may be generally referred to as a "casualty." Finally, a DOW is "a battle casualty who dies of wounds or other injuries received in action after reaching an MTF" (NATO 2010, 2-D-7).

The methodology only considers acute injuries that manifest within the time period during which operational and medical estimates are made (typically, 45 days or less).

The composite injury profile and the number of people for whom each injury profile applies are output from the human response component of the HRIP nerve agent methodology. This information is then used to determine casualty status as categorized by KIA, WIA, and DOW and to compile the resulting casualty estimates in a manner useful to the planner. The general criteria for use in the casualty estimation process are shown in Table 1.

KIA/DOW Estimation: Because the definitions of KIA and DOW rely on reaching an MTF, the first step in the casualty estimation process is defining the minimum time at which this can occur, measured relative to t_0. An individual can be assessed as KIA only if he/she dies during the time it takes to reach an MTF. An individual who dies after reaching an MTF is classified as a DOW. Before becoming a DOW, an individual would have previously been designated as a WIA.

An individual is classified as a fatality if his/her injury severity level has remained at Injury Severity Level 4 for 15 minutes. If this occurs before the time required to reach an MTF, the individual is considered KIA; otherwise, the individual is considered DOW.

WIA Estimation: An individual not already classified as a KIA is considered to be a WIA once his/her injury severity level is at or

Table 1. Casualty Estimation Process General Criteria

Type of Criteria	Value
Time to reach an MTF	Fixed time (recommended value: 30 minutes)
KIA	15 minutes at Injury Severity Level 4 occurring before reaching an MTF
WIA	First onset of symptoms at user-specified injury severity level (recommended value: Injury Severity Level 1)
DOW	15 minutes at Injury Severity Level 4 occurring after reaching an MTF

"Recommended" values are those values recommended by NATO subject matter experts(SMEs).
Credit: *Journal of Chemical Health and Safety* 18 (5) (2010).

exceeds the user-defined casualty threshold. WIAs are estimated using the composite injury profiles. An individual becomes a WIA at the point in time at which the severity of the composite injury profile—and therefore any one of his/her physiological symptoms—reaches the casualty threshold. In other words, if the injury profile severity at some time t is greater than or equal to the specified casualty threshold, the individual is classified as a WIA at time t.

Casualty Summation: The final step in the casualty estimation process is summarizing and reporting the casualty estimate. The methodology provides four types of output: population at risk (PAR), rates, profile, and flow. PAR is simply the total number of troops included in the scenario characterization. Rates provide the number of new casualties (KIA, WIA, and DOW) per 100 of the PAR each day. The profile demonstrates how the number of new casualties changes over time. Finally, the flow characterizes the movement between casualty categories (i.e., from WIA to DOW).

CONCLUSIONS

The HRIP nerve agent methodology provides a process for describing human response over time as a result of nerve agent exposure and using this information to estimate personnel status, including KIA, WIA, and DOW. The HRIP methodology is designed to support medical, operational, and logistical planners prepare for casualty-causing events.

The HRIP nerve agent methodology serves as a casualty estimation tool for planning purposes. It provides information on injury severity over time to facilitate the determination of casualty status. The methodology also allows the planner to set the criteria for determining when individuals become casualties—for example, by setting the injury severity level at which individuals become WIA. Finally, this methodology estimates casualties over time, allowing medical planners to estimate the flow of incoming patients and fatalities in the days and weeks following a CBRN event. Although this methodology is currently focused on military applications, could easily be adapted to civilian usage.

Since the completion of the HRIP model, IDA has been tasked to perform a number of follow-on efforts. These efforts include the development of HRIP parameters for additional CBRN agents and medical countermeasures, as well as the potential incorporation of the methodology into existing DoD models. IDA is also using the HRIP methodology as the basis for a new model designed to estimate the operational effects on military units exposed to CBRN agents and effects.

Dr. Disraelly, Ms. Walsh, Dr. Zirkle, and Dr. Curling are research staff members at IDA. Dr. Disraelly earned a doctorate in engineering management from The George Washington University. Ms. Walsh specializes in scientific programming and database architecture. Dr. Zirkle holds a doctorate in political science from the Massachusetts Institute of Technology. Dr. Curling holds degrees in environmental health science from the Harvard School of Public Health and in nuclear engineering from Rensselaer Polytechnic Institute.

The full article was published in the *Journal of Chemical Health and Safety.*

A NEW METHODOLOGY FOR ESTIMATING NERVE AGENT (SARIN (GB)/VX) CASUALTIES AS A FUNCTION OF TIME: DEFINING THE HUMAN RESPONSE INJURY PROFILE NERVE AGENT METHODOLOGY

http://www.sciencedirect.com/science/article/pii/S1871553210000927

REFERENCES

Disraelly, Deena S., Terri J. Walsh, Robert A. Zirkle, and Carl A. Curling. 2010. "A New Methodology for Estimating Nerve Agent (Sarin(GB)/VX) Casualties as a Function of Time: Implementing the Human Response Injury Profile Nerve Agent Methodology." *Journal of Chemical Health and Safety* 18 (5) (September–October): 5–11.

NATO. 2010. *Allied Administrative Publication 6 – NATO Glossary of Terms and Definitions.* Brussels.

NATO. 2002. *Allied Medical Publication 13 – NATO Glossary of Medical Terms and Definitions.* Brussels.

ROTORCRAFT SAFETY AND SURVIVABILITY

Mark A. Couch and Dennis Lindell

Finalist

This paper was based on an analysis of rotorcraft losses and fatalities sustained during Operation Enduring Freedom and Operation Iraqi Freedom (OEF/OIF) from October 2001 to September 2009. During this time frame, 375 rotorcraft losses with mishaps accounted for 81 percent of the losses, and aircraft shoot-downs accounted for the remaining 19 percent. These rotorcraft losses resulted in 496 rotorcraft fatalities, accounting for 71 percent of the fatalities. The remaining were due to aircraft shoot-downs. Compared to Vietnam, the OEF/OIF loss rate caused by aircraft shoot-downs was seven times lower due to reduced vulnerability (i.e., the inability of the aircraft to withstand a weapon hitting it) of many rotorcraft components to small-arms fire. The mishap loss rate was 2.72 losses per 100,000 flight hours, slightly exceeding the rotorcraft shoot-down loss rate. The in-theater mishap loss rate (Iraq and Afghanistan) was three times higher than the out-of-theater loss rate, with both exceeding the congressional and DoD goal of 0.5 mishaps per 100,000 flight hours.

The following article summarizes the paper "Study on Rotorcraft Safety and Survivability," published in the *Proceedings of the 66th American Helicopter International American Forum 2010,* Vol. 1.

Human factor mishaps accounted for 78 percent of all losses and 84 percent of all fatalities.

Combat hostile action losses include events where an airframe loss or fatal injuries to the crew or passengers occurred as a direct result of one or more threat weapons being fired at the aircraft. Combat non-hostile losses are Class A mishaps occurring within a recognized theater of combat operations (i.e., Vietnam, Desert Storm, OEF/OIF, etc.) in which the loss of aircraft or fatal injury to the crew or passengers is not a direct result of a threat weapon. Non-combat losses are Class A mishaps occurring outside a recognized theater of combat operations.

From October 2001 to September 2009, 375 rotorcraft losses resultes in 496 fatalities, as summarized in Table 1. Class A mishaps, which include both non-hostile and non-combat events, accounted for 305 losses, or 81 percent of all 375 rotorcraft losses, and combat losses (i.e., aircraft shoot-downs) accounted for the remaining 19 percent. Losses in a combat theater, which include the combat hostile action and non-hostile events, made up 61 percent of all losses and 73 percent of all fatalities. Table 1 also shows that loss and fatality rates in combat theaters were higher and are attributed to increased numbers of passengers on cargo and utility helicopter missions, acceptance of more operational risk on many missions, and routine exposure to combat threats.

Table 1. Rotorcraft Losses and Fatalities, October 2001 to September 2009: Hostile Action, Non-Hostile, Non-Combat, All Class A Mishaps

	Combat Hostile Action	Combat Non-Hostile	Non-Combat	All Class A Mishaps (Non-Hostile and Non-Combat)	All Combat Losses (Hostile and Non-Hostile)
Losses	70	157	148	305	227
Fatalities	145	219	132	351	364
Fatality/Loss Ratio	2.07	1.39	0.89	1.15	1.60
Loss Rate[a]	2.31	5.19	1.81	2.72	7.50
Fatality Rate[a]	4.79	7.24	1.61	3.13	12.03
Compared to DoD and Congressional Goals	7x lower[b]	10x higher[c]	4x higher[c]	5x higher[c]	–

[a] Per 100,000 flight hours

[b] Vis-à-vis Vietnam

[c] Vis-à-vis loss rate of 0.5 losses per 100,000 flight hours

COMBAT HOSTILE ACTION LOSSES

As a result of the extensive rotary wing combat hostile action losses in Vietnam, as shown in Table 2, the Army led an effort to significantly reduce the vulnerability of its helicopters to small arms and automatic weapons threats during the acquisition of the Utility Tactical Transport Aircraft System (UTTAS) and the Advanced Attack Helicopter (AAH). The UTTAS program required that the aircraft be capable of safe flight for at least 30 minutes after a single hit by a 7.62mm armor piercing incendiary (API) projectile striking anywhere on the aircraft. The AAH had more stringent requirements. The winning aircraft for the UTTAS program was the UH-60, and, for the AAH program, it was the AH-64. These two aircraft flew 60 percent of all rotary wing combat flight hours in OEF/OIF.

In the Vietnam and OEF/OIF conflicts, small arms and automatic weapons were the most prevalent threats hitting rotorcraft. During Vietnam, 94 percent of the combat hostile action losses and 80 percent of the fatalities were caused by small arms and automatic weapons, whereas in OEF/OIF, only 31 percent of the losses and 14 percent of the fatalities were caused by small arms and automatic weapons. The primary reasons for the decrease in small arms losses are the reduced vulnerability of the AH-64 and UH-60 and modified tactics that mitigated, but did not eliminate, the damage effects caused by small arms and automatic weapons. Table 2 shows that the total loss rate for all rotorcraft types is seven times lower, and the fatality rate is five times lower than Vietnam.

Table 2. Comparison of Rotorcraft Combat Hostile Action Losses from Vietnam to OEF/OIF

	Total Helicopters		Attack/Observation		Cargo/Utility	
	Vietnam	OEF/OIF	Vietnam	OEF/OIF	Vietnam	OEF/OIF
Losses	2,066	70	757	35	1,309	35
Fatalities	3,065	145	644	33	2,421	112
Fatality/Loss Ratio	1.48	2.07	0.85	0.94	1.85	3.20
Flight Hours	12,704,883	3,026,483	2,927,130	1,310,619	9,777,753	1,705,654
Combat Loss Rate[a]	16.26	2.31	25.86	2.67	13.39	2.05
Combat Fatality Rate[a]	24.12	4.79	22.00	2.52	24.76	6.57

[a] Per 100,000 flight hours

COMBAT NON-HOSTILE AND NON-COMBAT LOSSES

Table 1 also shows that the combat non-hostile mishap rate was ten times higher, and the non-combat loss rate was four times higher than the DoD and Congressional goal of 0.5 mishaps per 100,000 flight hours. When all mishaps are combined (both combat non-hostile and non-combat), the mishap loss rate was 2.71 losses per 100,000 flight hours, slightly higher than the loss rate due to combat hostile action of 2.31. Figure 1 shows the number of rotary wing Class A mishaps, destroyed aircraft, and fatalities by year using the bars and the left vertical axis. The significant increase in the number of fatalities compared to the number of Class A mishaps is directly related to the higher operational tempo associated with combat operations in Iraq and Afghanistan.

DoD mishap rates are defined as the number of mishaps per 100,000 flight hours and are typically reported for each fiscal year. Comparison of the fiscal year mishap rates is a method used by the Service safety centers to assess which communities are doing better or worse than others. However, use of the fiscal year reporting method sometimes creates an artificial binning of data that may show anomalies that are not statistically significant. To smooth out these possible anomalies, Figure 1 shows the 3-year mishap rates for all DoD aircraft, all fixed wing aircraft, tactical aircraft (TACAIR), and rotary wing, along with the DoD goal. Figure 1 shows that in general, from FY04 to FY08, the mishap rate trends downward. Reasons for the downward trending of the 3-year running average are the maturing of the OIF infrastructure; the maturing of the combat tactics, techniques, and procedures (TTP); and the drawdown in combat type of operations in Iraq in FY08 and FY09, which reduced operational risk. However, given the

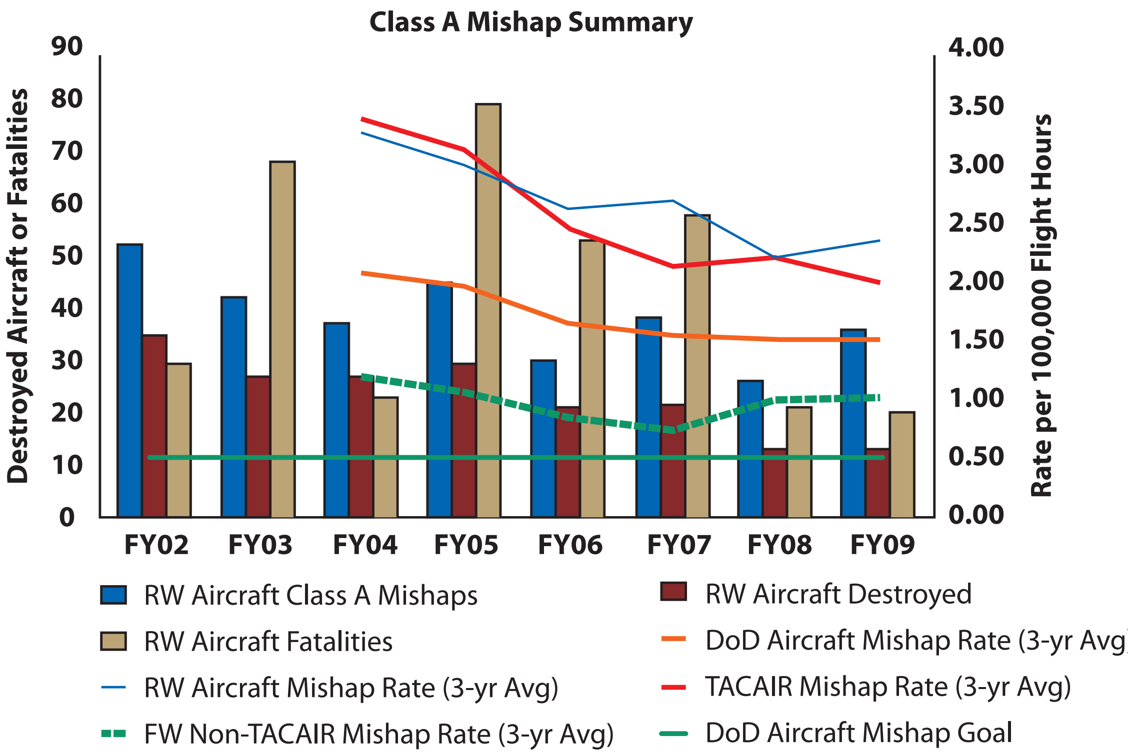

Figure 1. DoD Aircraft Class A Mishaps FY02–FY09

slope of this downward trending, it is unlikely that the all rotary wing mishap rate will meet the DoD goal of 0.5 mishaps per 100,000 flight hours anytime soon.

In the review of the mishap causal factors, two important trends were identified in mishap fatality data: the velocity at which the event occurred and whether the primary causal factor was a human factor or mechanical/material failure. Figure 2 shows the distribution of causal factors for losses and fatalities for both combat non-hostile and non-combat mishaps. The red and yellow slices of the pie charts indicate human factor mishaps. The red slices are human factor mishaps that occurred in cruise flight, while the yellow slices are human factor mishaps that occurred in hover or low speed, below effective translational lift. The blue slices indicate mishaps caused by mechanical or material failure, including engine failures, drive-train failures, and aircraft fires. The purple slices indicate flight-related mishaps, improperly forecasted weather, and undetermined mishaps that did not fit well into one of the other categories.

Human factor mishaps (red and yellow slices) accounted for 78 percent of all losses and 84 percent of all fatalities. The fact that more than three-quarters of the mishaps were human factor related does not necessarily mean that increased training or better supervision is required to reduce these types of mishaps. Although there were isolated cases where the root cause was a training or supervision failure, in many cases, the pilot lost situational awareness of his current

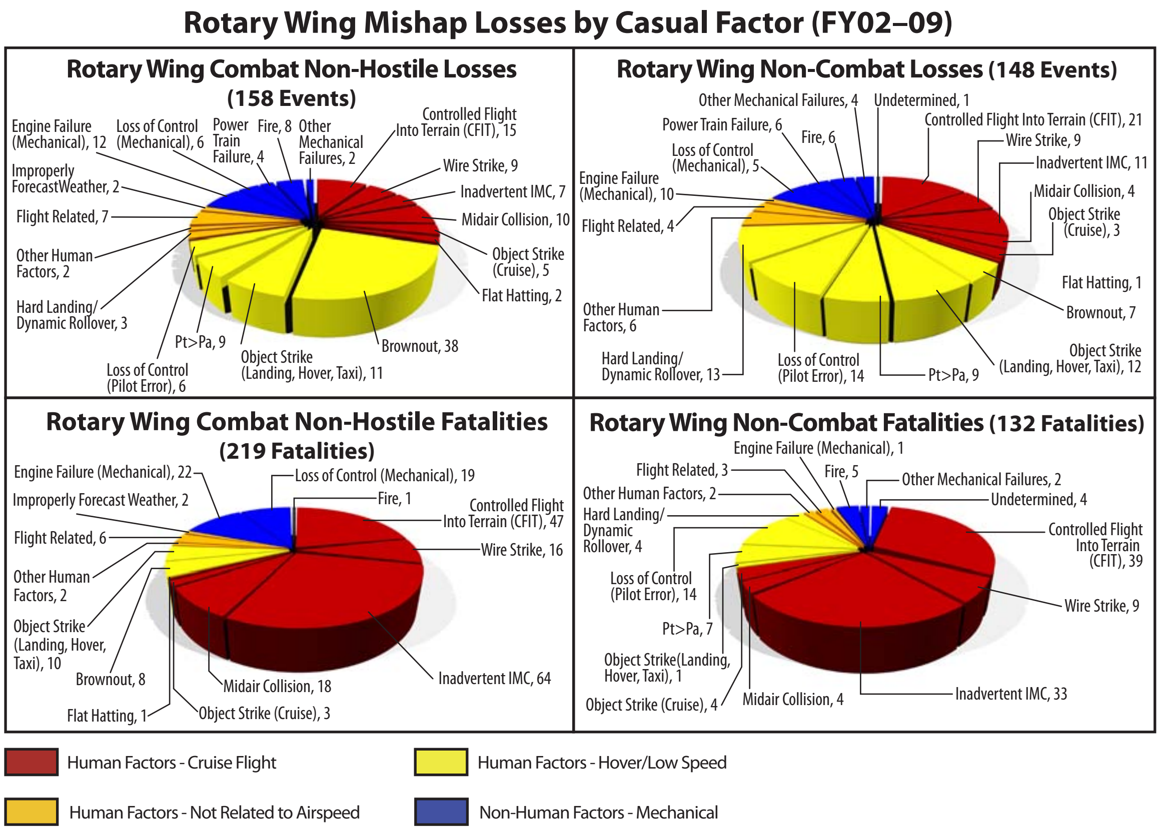

Figure 2. Rotary Wing Mishap Losses by Causal Factor (FY02–09)

flight/mission profile in relation to the surrounding terrain and obstacles. In other words, many mishaps occurred not because the pilots were inadequately trained, but because something kept them from being aware of the chain of events that were leading to the mishap.

KEY TECHNICAL FACTORS IMPACTING ROTORCRAFT LOSS RATES

Rotorcraft today are exposed to more lethal combat threats such as Man-Portable Air Defense Systems (MANPADS) and rocket-propelled grenades (RPGs). Technical concerns for combat hostile action losses include a lack of situational awareness during an attack, threat detection and jamming before the aircraft is hit, and damage tolerance after a hit. Technical concerns regarding rotorcraft mishaps include positional and situational awareness, warning for flight hazards and terrain, rapid response to hazards once detected, and component reliability. Furthermore, improved crashworthiness is applicable to combat threats and mishaps. Four concepts must be incorporated into the aircraft crashworthiness design to maximize the survival benefits: the design must maintain survivable living space; occupants must be restrained during the entire crash sequence; the aircraft and occupants must have a gradual deceleration during the crash sequence; and occupants must be able to egress the aircraft quickly after the crash.

APPLYING TACAIR LESSONS LEARNED

The prevailing perception is that TACAIR's improved survivability is the result of substantial and sustained research and development (R&D) investment in low observable technology, precision-guided standoff weapons and sensors, countermeasures, and electronic warfare. Improvements in TACAIR's capability and mission effectiveness since Vietnam center on tactics that limit or eliminate TACAIR's exposure to the most lethal threats. The primary lesson for rotorcraft is the value of technology, which allows tactics that limit exposure to their predominant threats to be modified. These technologies include susceptibility-reduction features such as lower infrared (IR), visual, and acoustic signatures; precision-guided standoff weapons and sensors; threat detection; and countermeasures. However, vertical lift missions will continue to require low-altitude flight in direct support of the ground forces. Therefore, vulnerability-reduction technologies, such as damage-tolerant components and fire protection/suppression, must still provide protection against threats in those profiles.

Figure 1 shows that the TACAIR mishap rate over the past 8 years is roughly the same as all rotary wing, with both exceeding the DoD goal of 0.5 mishaps per 100,000 flight hours. The primary technology difference between TACAIR and rotary wing is the use of fly-by-wire technology that make TACAIR capable of solutions not currently available to most rotorcraft. Fly-by-wire systems with advanced control laws have allowed TACAIR to expand the flight envelope, enable automatic avoidance of hazards, and increase aircraft survivability.

PRIORITIZING ROTORCRAFT SOLUTIONS

Two mishap causes and two threat weapon categories accounted for most of the loss of life and airframes from October 2001 through September 2009. They were controlled flight into terrain (CFIT), degraded visual environment (i.e., brownout), guided weapons, and ballistic weapons. Reducing the impact of these four primary causal factors could significantly improve the safety and survivability of the DoD rotary wing fleet. Table 3 lists the candidate solutions for reducing rotorcraft losses.

CONCLUSIONS

Rotary wing aircraft are and will continue to be critical to the warfighter. Losses and fatalities by any cause will have a substantial impact on operations. Implementation of the following recommendations will reduce the number of rotorcraft losses and fatalities, allowing US combat forces to operate effectively in any environment.

1. To reduce combat losses further, increase and sustain the investment to improve rotorcraft situational awareness, threat detection and jamming, and damage tolerance (vulnerability reduction).

2. To meet the goal of 0.5 mishaps or less per 100,000 flight hours, increase and sustain the investment in rotorcraft positional and situational awareness; warning for flight hazards, terrain, and obstructions; rapid response to hazards once detected; advanced engine and power train technology; and improved component

Table 3. Candidate Solutions for Reducing Rotorcraft Losses

Loss Category	Focus Areas	Candidate Solutions
Controlled flight into terrain (cruise flight)	Improved awareness: Decreased pilot workload:	Terrain warning (w/digital database) Real-time weather updates combines with a terrain avoidance warning system Low-power radar for obstacle detection Advanced flight control systems
Degraded visual environment (low speed and hover)	Improved awareness: Decreased pilot workload: Improved facilities: Improved crashworthiness:	Flight displays w/low speed flight symbology Advanced flight control systems Simulator and Training area realism and availability Updated crashworthiness criteria Improved occupant seats and restraints
Guided Weapons (MANPADS, RF/IR missiles)	Improved awareness: Improved countermeasures: Reduced vulnerability: Improved crashworthiness:	Missile warning Integrated aircraft survivability equipment Improved IR countermeasures and expendables (new research, more capacity) Fire protection Updated crashworthiness criteria Improved occupant seats and restraints
Ballistic Projections (RPGs, rockets, and small arms/automatic weapons	Improved awareness: Improved countermeasures: Reduced vulnerability: Improved crashworthiness:	Unguided threat detection Integrated aircraft survivability equipment Optical jamming/dazzling Fire protection Ballistic protection Updated crashworthiness criteria Improved occupant seats and restraints

reliability. Advanced flight control systems that use modern control features, such as fly-by-wire, are key enabling technologies.

3. To reduce personnel injuries and fatalities for combat threat losses and mishaps, improve airframe crashworthiness and crash protection for passengers. DoD crashworthiness standards have not been updated since the 1970s and need to be expanded in scope to cover a wider set of aircraft and environmental conditions.

Dr. Couch is a research staff member at IDA. He earned his doctorate in aeronautical and astronautical engineering from the Naval Postgraduate School. Mr. Lindell is the Manager of the Joint Aircraft Survivability Program (JASP). He received his B.S. in aerospace engineering and mechanics from the University of Minnesota.

The full article was published in the *Proceedings of the 66th American Helicopter International Annual Forum 2010*, Vol. 1.

PROBE OF CHOPPER LOSSES GAINS ATTENTION

http://www.vtol.org/what-we-do/safety

SECURE CLOUD BASED COMPUTING

Coimbatore Chandersekaran, William R. Simpson, and Ryan R. Wagner

Finalist

Cloud computing is emerging as an attractive, cost-effective computing paradigm. However, as currently implemented, cloud services do not meet the high assurance requirements of defense, banking, credit, and content-distribution organizations, among others. High assurance computing provides protection of information assets, accountability, confidentiality, integrity, and availability under adverse conditions and in the presence of malicious threats. These requirements strain the limits of traditional computing and necessitate a number of mechanisms related to high assurance to address the issue. This paper will describe the high assurance challenges and possible solutions to them. The challenges are primarily in four areas: virtualization and the loss of attribution that accompanies the cloud environment; the inability to perform end-to-end communications; the need for a comprehensive key management process; and monitoring and logging for attribution, compliance, and data forensics.

The following article summarizes the paper "High Assurance Challenges for Cloud Based Computing," which appeared in the *Proceedings of the World Congress on Engineering and Computer Science 2011,* Vol. I.

Cloud computing has come to mean many different things. To some, it is simply putting data on a remote server. However, this paper uses the definition provided by National Institute for Standards and Technology (NIST). It defines five essential characteristics of any cloud computing environment:

1. On-demand self service,
2. Broad network access,
3. Resource pooling,
4. Rapid elasticity, and
5. Measured service.

Cloud computing has come to mean many different things. To some, it is simply putting one's data on a remote server.

Significantly, multi-tenancy and virtualization are not essential characteristics for cloud computing. For this discussion, we will assume neither multi-tenancy nor virtualization since the latter adds the most efficiency in terms of minimizing resources and cost while adding operational flexibility. The arguments that follow do not require either trait. Cloud computing is, at its core, a service that is characterized by three primary models. In the lowest level, Infrastructure as a Service (IaaS), storage, computation, and networking are provided by the cloud provider to the cloud consumer. In the next level, Platform as a Service (PaaS), all the trappings of IaaS plus an operating system and perhaps some application programming interfaces (APIs) are provided and managed by the cloud provider. In the highest service, Software as a Service (SaaS), the cloud provider offers an end-user service such as web mail. As the level of service increases, the cloud provider gains more control over who can access information and how it can be modified or shared, and the cloud consumer has less control.

Cloud services are deployed using four models that are primarily either public or private. In a public cloud, the infrastructure—although generally not the data on it—can be used by anyone agreeing to its terms of use. Public clouds exist off the premises of the cloud consumer. Private cloud infrastructure is used by only one organization and can exist on or off the organization's premises. Each infrastructure has two variations. In a community cloud, a group of organizations with similar interests or needs share a cloud infrastructure that is not open to the general public. In a hybrid cloud, two or more cloud deployment models are connected in a way that allows data or services to move between them. One example would be an organization's private cloud that uses a community cloud during periods of high use.

HIGH ASSURANCE COMPUTING

While current implementations of cloud computing provide efficient and operationally friendly solutions to data computing and content distribution, they fail to meet high assurance standards.

In certain enterprises, the network assets are of such high value (monetary or other value) that attacks (from outside or within the enterprise) are mounted to gain control of the network, its assets, or both. This omnipresent threat leads to a healthy paranoia of intercept, masquerade, and threats that are resistant to observation. Despite this hostile environment, the web interface is the best way for users to gain network access. One way to continue operating in this environment is to know and vet not only your users, but also your software and devices. However, even these precautions are not fail proof in an environment of voluminous threats. Today, we regularly construct seamless encrypted communications between machines through a Secure Sockets Layer (SSL) or other Transport Layer Security (TLS), but these layers do not protect the "last mile," the transport portion between the machine and the user (or service) on one end and the machine and the service on the other end. Securing this last mile is particularly problematic since malware may exist on either machine, opening the transactions to eavesdropping, exfiltration, session high-jacking, data corruption, man-in-the-middle, masquerade, blocking or termination of service, and other nefarious behaviors.

Before examining the challenges of cloud computing systems, let us first examine the eight architectural elements of high assurance computing: naming and identity, credentials, public key infrastructure (PKI), certificate services, bilateral end-to-end authentication, authorization using Security Assertion Markup Language (SAML) packages, registration of the Security Token Server (STS), and recognizing STS signatures. These elements ensure that security is built into the systems. In the architecture we espouse, the basic formulation follows web 2.0 and uses Organization for the Advancement of Structured Information Standards (OASIS) standards of security. These elements are explained below.

Naming and Identity: Identity is established by the requesting agency. In the DoD, this is primarily through the Electronic Data Interchange Personal Identifier (EDIPI). To avoid a collision between the EDIPI and the identity used by all federated exchanges, the DoD uses Distinguished Name (DN) as it appears on the primary credential provided by the certificate authority. Since the DN must be unique over time and space, retired names are not reused, and names that appear duplicative are eliminated. All active entities (persons, machines, and software) must be uniquely named.

Credentials: Each identity (all active entities) requiring access is credentialed by a trusted credentialing authority. Further, an STS must be used for storing attributes associated with access control. The STS used for generating SAML tokens must also be credentialed (primarily through the same credentialing authority), although others may be entertained.

PKI-required X.509 Certificates: The PKI embodied in an X.509 certificate is the primary exchange medium for setting up authentication of identities and setting up crypto-graphic flows.

Certificate Services: The certificate authority must use known and registered (or, in specific cases, defined) certificate-revocation and currency-checking software.

Bilateral End-to-End Authentication: To begin, the requestor authenticates to the service (not the server), and the service authenticates to the requestor. This two-way authentication avoids a number of threat vulnerabilities. The requestor also authenticates to the server and sets up a TSL connection to begin communication with the service. Public keys in the X.509 are the primary method of authentication. The keys can then be used to set up encrypted communications, either by X.509 keys or a generated session key. Simple Object Access Profile (SOAP) envelopes are the preferred method of secure communication. All messages are encrypted for delivery to the recipient.

Authorization Using SAML Packages: All authorizations are through the use of SAML packages in accordance with the SAML 2.0 specification provided by OASIS.

Registration of the STS: All STSs that create and sign SAML packages must be registered. The certificate of the STS is used to sign SAML tokens and to complete bilateral authentication between requestors and the STS.

Recognizing STS Signatures: STS signatures are recognized only for registered STSs and may be repackaged by the local STS after registration. Unrecognized signatures are not honored and, once refused, are logged as a relevant security event.

CHALLENGES IN COMBINING THE CLOUD AND HIGH ASSURANCE

Despite the obvious advantages of cloud computing, its reliance on virtualization and redirection pose a number of problems for high assurance. To understand this problem, let's examine a security flow in a high assurance system. The application system consists of a web application (for communication with the user) and at least one aggregation service that invokes one or more exposure services and then combines the services' information for return to the web application and the user. As a pre-requisite to end-to-end communication, an SSL or other suitable TLS is set up between each machine. The exposure services retrieve information from one or more Authoritative Data Sources (ADSs). Each communication link in Figure 1 is authenticated end to end with the use of public keys in the X.509 certificates, which are provided for each active entity.

This two-way authentication avoids a number of threat vulnerabilities. Once the authentication is completed, an SSL/TLS connection is established between the requestor and the service provider. Within the connection pipe, which is encrypted, a Web Service

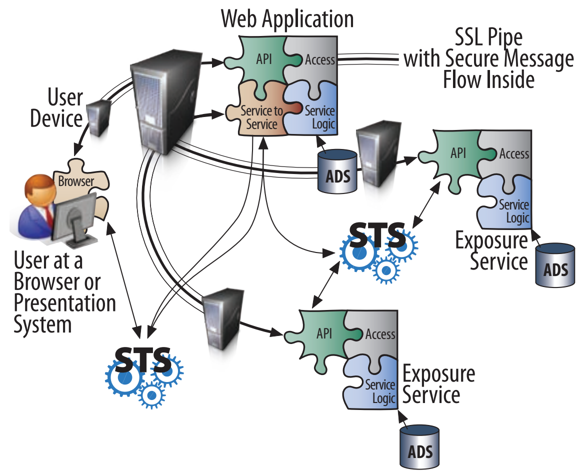

Figure 1. High Assurance Security Flows

(WS)[1]-Security package is sent to the service. The WS-Security package contains a SAML token generated by the STS in the requestor domain. Public keys in the X.509 certificate are the primary method of authentication. The certificate can then be used to set up encrypted communications (either by X.509 keys or a generated session key). Session keys and certificate keys need to be robust and sufficiently protected to prevent malware exploitation. The preferred method of communication is secure messaging using WS-Security, contained in SOAP envelopes. The public key of the target is used as the encryption key, ensuring that only the target can interpret the communication.

Cloud environments and virtualization are attractive because they address scale-up and performance problems. The cloud delivers assets and retires them as needed. Examining scaling up in a secure environment that does not use cloud technologies shows only the web application, although the same rules (end-to-end authentication and SAML-based access

[1] Web Service as defined in OASIS standards.

control) apply to all communication links between any active elements shown in Figure 2. The simplest way to divide the load is to stand up multiple independent instances and divide users into groups that will use the various instances. Dependent instances that extend the thread capabilities of the server are considered single independent instances. Figure 2 shows a representation that approximates the cloud environment. A traffic monitor (load balancer) watches for activity and posts a connection to an available instance. This case works well because the new instance has a unique name, end-to-end encrypted communication with SAML delivery to the end point, and credentials to proceed. All of this activity, of course, needs to be logged in a standard form, and parameters must be met so that forensic specialists can easily reconstruct the instance. We have shown a couple of threats where an eavesdropper may actually try to insert himself in the conversation (man-in-the-middle). These instances need mitigation. Another example, instance 4, highlights the need to protect caches and memory spaces.

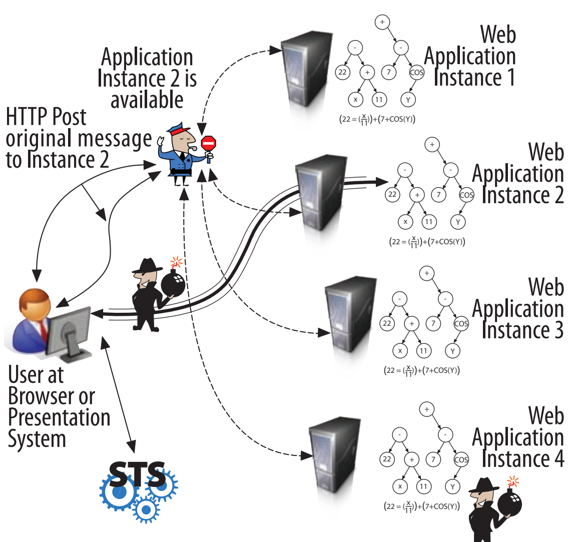

Figure 2. High Assurance Load Balancing

When a cloud environment runs out of resources for computing, it builds additional instances. Some may be thread extension schemas, and some may be independent instances. The traffic monitor here is often called a hypervisor, and it keeps track of the instances and connections. Figure 3 shows notionally how this operation would work. When thread capacity is saturated at the server, the hypervisor would nominally redirect the request to an independent virtual or real instance of the web application. If none exists, it would build one from elements in the resource pool, as depicted in instance 4 on the chart. If the last user signs off of an independent virtual or real instance (instance 3 in Figure 3), the hypervisor would tear down the instance and return the resources to the resource pool. This result would provide an efficient reallocation of resources.

Several steps must be taken to preserve the security of a high assurance computing environment. The number of independent instances must be anticipated. Names, credentials, and end points must be assigned according to their uses. The attribute stores must be provisioned with properties for the names in the credentials, and keys must be present in the hardware storage modules to be used in the authentication process. The simple redirect must be changed to a repost loop, as in Figure 2. The user will then have a credentialed application with which to authenticate bilaterally and an end point for end-to-end message encryption. Key management is complex and essential. When a new independent instance is required, it must be built and activated (credentials and

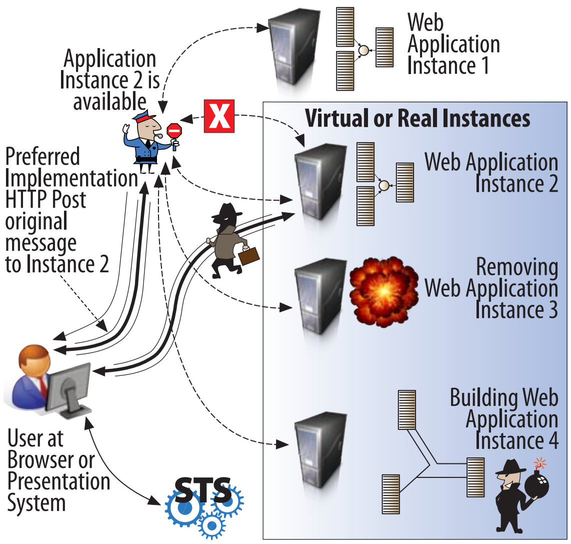

Figure 3. High Assurance Virtualized Hypervisor Activity

properties in the attribute store, as well as the end point assignment). All these activities must be logged in a standard format with reference values that facilitate reassembling the chain of events for forensics. When a current independent instance is retired, it must be disassembled and deactivated (credentials and properties in the attribute store, as well as end point assignment). All these activities must be logged in a standard format with reference values that make it easy to reassemble the chain of events for forensics. The same threat environment exists, and the same safeguards must be taken. In fact, in Figure 3, nefarious code is built right into the virtual or real instance 4, a problem that underscores the need for trusted and verified software to do the virtualization and protection of the resources in the resource pool.

SUMMARY

We have reviewed the basic approaches to clouds and their potentials for savings in computing environments. We have also discussed one high assurance architecture and its requirements that directly challenge the way cloud computing environments are organized. Notably, the extensive use of virtualization and redirection is so widespread that many customers who need high assurance have rejected the concept of cloud computing. We believe, however, that precisely identifying the high assurance requirements can lead to solutions in the cloud computing environment and can expand the technology's potential uses.

Mr. Chandersekaran, Dr. Simpson, and Mr. Wagner are research staff members at IDA. Mr. Chandersekaran earned a master's in electrical engineering from the Indian Institute of Technology. Dr. Simpson earned a doctorate in aerospace engineering from The Ohio State University. Mr. Wagner earned a master's in electrical engineering and computer science from the Massachusetts Institute of Technology.

The full article was published in *Proceedings of the World Congress on Engineering and Computer Science 2011,* Vol. I.

CLEARING OBSTACLES ASSOCIATED WITH CLOUD COMPUTING

http://www.iaeng.org/publication/WCECS2011/WCECS2011_pp61-66.pdf

REFERENCES

Catteddu, Daniele, and Giles Hogben. November 2009. *Cloud Computing Risk Assessment*. Greece: Heraklion – Crete: European Network Information Security Agency (ENISA). http://www.enisa.europa.eu/act/rm/files/deliverables/cloud-computing-risk-assessment.

Chandersekaran, Coimbatore, and William R. Simpson. 2010. "A SAML Framework for Delegation, Attribution, and Least Privilege." *In Proceedings of the 3rd International Multi-Conference on Engineering and Technological Innovation: IMETI 2010*, Vol. 2, 303–308. Orlando, FL, June 29–July 2.

Chandersekaran, Coimbatore, William R. Simpson, and Ryan R. Wagner. 2011. "High Assurance Challenges for Cloud Computing. " In *Proceedings World Congress on Engineering and Computer Science 2011*, Vol. I, 61–66. San Francisco, CA, October 19–21.

Chrapaty, Debra. 2008. Remarks at the Microsoft Management Summit. Las Vegas, NV, May 1. http://www.microsoft.com/Presspass/exec/debrac/mms2008.mspx.

Cloud Security Alliance. December 2009. *Security Guidance for Critical Areas of Focus in Cloud Computing V2.1*. https://cloudsecurityalliance.org/csaguide.pdf.

Jansen, Wayne, and Timothy Grance. January 2011. *Guidelines on Security and Privacy in Public Cloud Computing*. NIST Report SP 800-144 (Draft). Gaithersburg, MD: Security Division, Information Technology Laboratory, National Institute of Standards and Technology. http://csrc.nist.gov/publications/drafts/800-144/Draft-SP-800-144_cloud-computing.pdf.

Johnson, Bobbie. "Cloud Computing Is a Trap, Warns GNU Founder Richard Stallman." *The Guardian*, September 29, 2008. http://www.guardian.co.uk/technology/2008/sep/29 /cloud.computing.richard.stallman.

Mell, Peter, and Timothy Grance. January 2011. *Cloud Computing*. NIST Report SP 800-145 (Draft). Gaithersburg, MD: Computer Security Division, Information Technology Laboratory, National Institute of Standards and Technology. http://csrc.nist.gov/publications/drafts/800-145/Draft-SP-800-145_cloud-definition.pdf.

OASIS Identity Federation. *Liberty Alliance Project*. http://projectliberty.org/resources/specifications.php.

OASIS. March 2005. *Profiles for the OASIS Security Assertion Markup Language (SAML) V2.0*. http://docs.oasis-open.org/security/saml/v2.0/saml-profiles-2.0-os.pdf.

Plesser, Andy. "Cloud Computing is Hyped and Overblown, Forrester's Frank Gillett.....Big Tech Companies Have 'Cloud Envy.'" *Beet TV*, September 26, 2008. http://www.beet.tv/2008/09/cloud-computing.html.

Simpson, William R., and Coimbatore Chandersekaran. 2009. "Information Sharing and Federation." In *Proceedings of the 2nd International Multi-Conference on Engineering and Technological Innovation: IMETI 2009*, Vol. I, 300–305. Orlando, FL, July 10–13.

Simpson, William R., Coimbatore Chandersekaran, and Andrew Trice. 2008. "Cross-Domain Solutions in an Era of Information Sharing." In *Proceedings of the 1st International Multi-Conference on Engineering and Technological Innovation: IMETI 2008*, Vol. I, 313–318. Orlando, FL, June 29–July 2.

Simpson, William R., Coimbatore Chandersekaran, and Andrew Trice. 2008. "A Persona-Based Framework for Flexible Delegation and Least Privilege." Briefing presented at the *20th Annual System and Software Technology Conference*. Las Vegas, NV, April 29–May 2.

Standard for Naming Active Entities on DoD IT Networks, Version 3.5. September 23, 2010.

ORBITAL MANEUVER OPTIMIZATION USING TIME-EXPLICIT POWER SERIES

James D. Thorne

The availability of previously published explicit time series solutions to the classical Lambert orbit determination problem allows for the total change in velocity associated with a series of orbital maneuvers to be expressed as an algebraic function of the individual transfer times only. The algebraic objective function is then minimized for a series of maneuvers by finding the optimal transfer times for each of the orbital arcs.

The following article summarizes the original paper, "Orbital Maneuver Optimization Using Time-Explicit Power Series." Originally published in *Celestial Mechanics and Dynamical Astronomy*, the paper presents an example of the optimization technique as applied to an interplanetary flyby mission to the asteroids Pallas and Juno in a fixed total mission time of 7 years.

Orbital maneuver optimization as a function of the transfer time is traditionally accomplished using either classical calculus of variations techniques for restricted cases or by direct numerical sampling to minimize the magnitude of the required changes in velocity vectors (Δv). However, numerical sampling will not guarantee optimality and can offer only limited insight into the qualitative behavior of the system either inside or outside of the assigned search space. To find the required velocity components before and after each maneuver point with specified transfer times, one must somehow solve the Lambert orbit determination problem for each transfer arc. Lambert's Theorem states that there is a unique value of the semi-major axis, a, associated with the arc of a *single* conic section that will correspond to a given flight time, t, and the given problem geometry. The Lambert problem can be expressed in terms of the Lagrange trajectory equations, which equate the transfer time t to transcendental functions of the unknown semi-major axis. Recently, time series solutions have been found (Thorne 2004, 441; Vallado 2007, 476) to solve all orbital cases of the Lambert problem by analytically reversing the functional dependence of the Lagrange trajectory equations from a to t, which allows for the total Δv magnitude for a series of orbital maneuvers to be written as a single *algebraic* expression, an explicit function of only the individual transfer times. By truncating the resulting power series terms to achieve the desired accuracy, these solutions can be used as polynomial functions for the unknown a of each orbital transfer arc. The Δv function can then be minimized for a series of sequential maneuvers by finding the set of optimal flight times for each of the individual orbital transfer arcs. The total change in velocity is the sum of n vector differences. The goal is to minimize the objective function, J, which is the sum of the magnitudes of the total number of the velocity changes in the orbital mission:

$$J = \sum_{n=1}^{total} \Delta v_n = \begin{array}{l} \sqrt{(\dot{x}_1 - \dot{x}_0)^2 + (\dot{y}_1 - \dot{y}_0)^2 + (\dot{z}_1 - \dot{z}_0)^2} + \ldots + \\ \sqrt{(\dot{x}_{2n-1} - \dot{x}_{2n-2})^2 + (\dot{y}_{2n-1} - \dot{y}_{2n-2})^2 + (\dot{z}_{2n-1} - \dot{z}_{2n-2})^2}. \end{array} \quad (1)$$

One way to find the velocity at the n^{th} point in the orbit is to use the Lagrange coeffcient functions f, g and their time derivatives (Battin 1987, 128). Here is an example using the two cartesian coordinates, x and y:

For n maneuvers, the velocity components are

$$\dot{x}_{2n-1} = \frac{1}{g_n} x_{n+1} - \frac{f_n}{g_n} x_n, \quad (2)$$

$$\dot{y}_{2n-1} = \frac{1}{g_n} y_{n+1} - \frac{f_n}{g_n} y_n, \quad (3)$$

$$\dot{x}_{2n} = \dot{f}_n x_n + \dot{g}_n \dot{x}_{2n-1}, \quad (4)$$

$$\dot{y}_{2n} = \dot{f}_n y_n + \dot{g}_n \dot{y}_{2n-1}, \quad (5)$$

where the Lagrange coeffcient functions f_n, g_n, $\dot{f}_n$, $\dot{g}_n$ are given by

$$f_n = 1 - \frac{a_n}{r_n}\left(1 - \cos\left(\Delta E_n\right)\right), \quad (6)$$

$$g_n = t_n - \sqrt{\frac{a_n^3}{\mu}}\left(\Delta E_n - \sin\left(\Delta E_n\right)\right), \quad (7)$$

$$\dot{f}_n = -\frac{\sqrt{\mu a_n}}{r_n r_{n+1}} \sin(\Delta E_n), \quad (8)$$

$$\dot{g}_n = 1 - \frac{a_n}{r_{n+1}}\left(1 - \cos(\Delta E_n)\right). \quad (9)$$

The change in eccentric anomaly, ΔE_n, can be found by using the Lagrange parameters α_n and β_n, depending on the type of orbit transfer. For arcs of ellipses, the four possibilities are

1A: ($\theta < 180°$, short way)	$\Delta E_n = \alpha_n - \beta_n$
1B: ($\theta < 180°$, long way)	$\Delta E_n = 2\pi - \alpha_n - \beta_n$
2A: ($\theta > 180°$, short way)	$\Delta E_n = \alpha_n + \beta_n$
2B: ($\theta > 180°$, long way)	$\Delta E_n = 2\pi - \alpha_n + \beta_n$

(10)

The Lagrange parameters are defined as follows (Battin 1987, 278):

$$\alpha_n = 2\sin^{-1}\sqrt{\frac{s_n}{2a_n}}, \quad \beta_n = 2\sin^{-1}\sqrt{\frac{s_n - c_n}{2a_n}}, \quad (11)$$

where a_n is the semi-major axis of the n^{th} transfer orbit and μ is the gravitational constant. The hyperbolic cases are similar. It has been shown previously (Thorne 2004, 447) that the series solution for both the hyperbolic and short-way elliptic transfer type (A) is given by

$$a = \left(\frac{s}{2}\right) \sum_{k=0}^{\infty} \underset{[\text{H,A}]}{B_k} \left(\frac{t}{t_p} - 1\right)^{(k-1)}, \quad (12)$$

where t_p is the parabolic transfer time for the given geometry and the $\mp$ signs correspond to transfer angles of less than or greater than 180 degrees, respectively:

$$\text{1P, 2P:} \quad t_p = \frac{1}{3}\sqrt{\frac{2s^3}{\mu}}\left[1 \mp \left(\frac{s-c}{s}\right)^{3/2}\right]. \quad (13)$$

The series solution for long-way transfers (B) near the minimum-energy time is given by (Thorne 2004, 448):

$$a = \frac{s}{2} + del^2, \; del = \sum_{k=1}^{\infty} \underset{[\text{B-me}]}{B_k} (t - t_{me})^k, \quad (14)$$

The solution for the long-way elliptic case (B) as the transfer time approaches infinity is (Thorne 2004, 450)

$$a = \sum_{k=0}^{\infty} \underset{[\text{B- inf}]}{B_k} \, t^{\left(\frac{2-k}{3}\right)}. \quad (15)$$

Although all of the B_k coeffcients in these series equations are functions of the problem geometry, they differ by orbit transfer type (Thorne 2004, 451).

As defined in Eq. (1), J is a function of the velocity vector, $\vec{v}$, which is the first time derivative of $\vec{r}$, as follows:

$$J = J(\vec{v}) \qquad (16)$$

The velocity components are functions of the f and g expressions and their time derivatives, and the components of the position vectors that are given constants. Denoting this group of expressions by f, we have:

$$J = J(\vec{v}(f)) \qquad (17)$$

The f and g expressions and their time derivatives are functions of a_n, t_n and ΔE_n, so J becomes

$$J = J(\vec{v}(f(a_n, t_n, \Delta E_n))) \quad (18)$$

Finally, ΔE_n is a function of a_n, and a_n is a time series in t_n, so J can be expressed as a single algebraic function of t_n as follows:

$$J = J(\vec{v}(f(\Delta E_n (a_n (t_n))))) \quad (19)$$

Starting with Eq. (1), one can substitute Eqs. (2) through (15) as appropriate into J to produce an algebraic function of only the transfer times, t_n, and known constants. J can be minimized numerically with respect to the t_n with little difficulty. The following example is taken from a proposed flyby mission to the sun-orbiting asteroids Pallas and Juno, starting from earth parking orbit. The orbits of Pallas and Juno are inclined, but the transfer arcs are shown as projections onto the plane of the ecliptic in Figure 1.

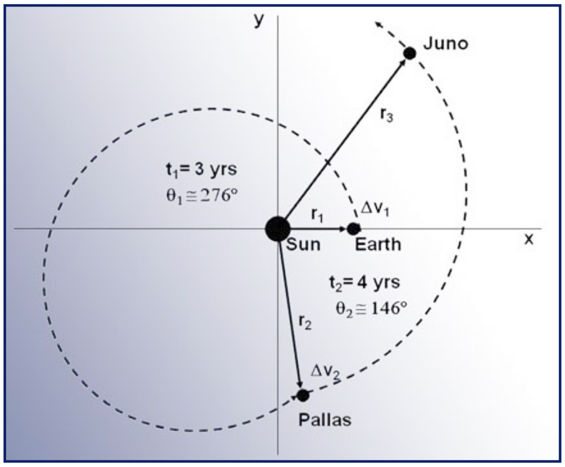

Figure 1. Reference Case for Earth-Pallas-Juno Flyby Mission in the X-Y Plane

The initial position vector has a magnitude of one astronomical unit (AU), and the gravitational constant is normalized to unity. This example has an additional constraint that the sum of the two transfer times must be equal to 7 years, with a reference case of t_1 = 3.0 years and t_2 = 4.0 years. Figure 1 shows the reference case. Because of the constraint that $t_2 = 7 - t_1$, the only independent variable in the objective function J is t_1, after substitution. To do the minimization analytically, the unknown semi-major axis of each of the two transfer arcs must be expressed as a time series. The following equations show the numerical values of the first few coefficients of the series for each of the two unknown semi-major axis. A total of 15 series terms were used as before. The numerical values can be produced from the given problem geometry using recursive relationships (Thorne 2004, 451). To find a_1 for the first transfer, the argument of the series is $T_1 = (t_1/t_{p1} - 1)$ for use in Eq. (12):

$$
\begin{aligned}
a_1 \;=\;& 0.606326779 \times T_1^{-1} + 1.082815477 \times T_1^0 + 0.405850843 \times T_1^1 - 0.044185431 \times T_1^2 \\
& + 0.013667178 \times T_1^3 - 0.005757163 \times T_1^4 + 0.002842438 \times T_1^5 - 0.001549493 \times T_1^6 \\
& + 0.000904783 \times T_1^7 - 0.000556037 \times T_1^8 + 0.000355637 \times T_1^9 + \ldots . \qquad (20)
\end{aligned}
$$

For a_2 , the series solution is given by Eq. (15).

$$
\begin{aligned}
a_2 \;=\;& 0.293683865 \times t_2^{(2/3)} + 0.0 \times t_2^{(1/3)} + 0.0 \times t_2^{(0/3)} + 1.335329741 \times t_2^{(-1/3)} + 0.0 \times t_2^{(-2/3)} \\
& + 4.166086492 \times t_2^{(-3/3)} - 1.517878345 \times t_2^{(-4/3)} + 22.854605878 \times t_2^{(-5/3)} \\
& - 28.413712080 \times t_2^{(-6/3)} + 133.130239337 \times t_2^{(-7/3)} - 333.662978219 \times t_2^{(-8/3)} + \ldots , \qquad (21)
\end{aligned}
$$

where $t_2 = 7 - t_1$. In canonical units, one year is equal to 2π time units, so the constraint becomes $t_2 = 14\pi - t_1$.

Figure 2 shows the trajectories for the lowest Δv case found in this analysis. The asteroid Pallas is in the position it would have been after 2 years of normal propagation, but the transfer times have been allowed to vary independently. The total trip time was still fixed at 7 years, regardless of the initial launch time that would be required to achieve the desired geometry.

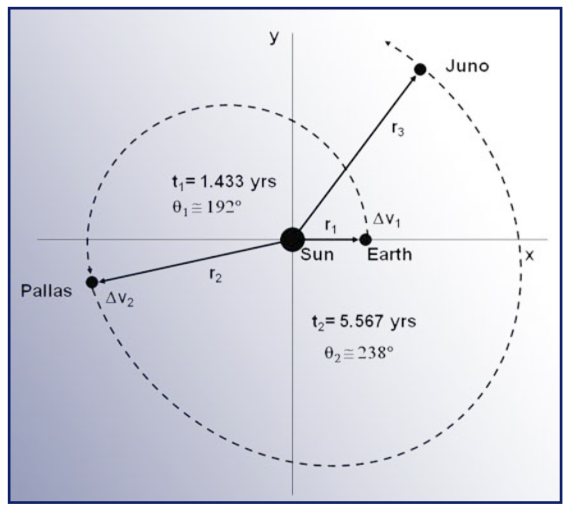

Figure 2. Low Delta-V Case for Earth-Pallas-Juno Flyby Mission in X-Y Plane

With a complete set of series solutions available for every case of the Lambert problem, it is possible to optimize multiple-impulse missions to minimize total fuel requirements using analytical methods. Since the semi-major axis can be approximated as a polynomial in transfer time by truncating the infinite series solutions to a desired order, the transfer time itself may then appear explicitly in an expression for change in orbital velocities. The resulting algebraic expression can then be minimized over the complete set of transfer times.

Dr. Thorne is a research staff member at IDA. He holds a doctorate in astronautical engineering from the Air Force Institute of Technology.

The full article was published in the journal *Celestial Mechanics and Dynamical Astronomy.*

ASTRODYNAMICS RESEARCH DESIGNED TO MINIMIZE FUEL BURNED

http://link.springer.com/article/10.1007%2Fs10569-011-9336-4

REFERENCES

Battin, R. H. 1987. *An Introduction to the Mathematics and Methods of Astrodynamics*. New York: AIAA Education Series.

Thorne, J. D. 2004. "Lambert's Theorem – A Complete Series Solution." *The Journal of the Astronautical Sciences* 52 (4) (October/December): 441–454.

Thorne, J. D. 2011. "Orbital Maneuver Optimization Using Time-Explicit Power Series." *Celestial Mechanics and Dynamical Astronomy* 110 (1) (May): 31–42.

Vallado, D. A. 2007. *Fundamentals of Astrodynamics and Applications*. El Segundo, CA: Microcosm Press.

PREDICTED AND MEASURED MULTIPATH IMPULSE RESPONSES

Kent Haspert and Michael Tuley

The fundamental concepts used to evaluate multipath effects date back over 50 years. Today's technology can support wide-bandwidth communications and radar systems that were not available or considered when these multipath concepts were being formulated.

The following article summarizes a slightly modified version of the original analytical approaches for evaluating multipath effects and compares the predicted multipath to data collected from a wideband instrumentation radar. The multipath model presented here covers the specular (coherent) and the diffuse (noncoherent) components of multipath. The test data were collected for conditions that strongly favor diffuse multipath, but the experimental technique supported detection of any unanticipated specular contributions. Because the purpose of this validation effort was to perform an in-depth examination of multipath effects, the demanding test conditions revealed a couple of real-world effects that had to be addressed. After incorporating these effects into the analytical multipath formulations, IDA was able to show very close agreement between the predicted and observed multipath.

Finalist

The multipath model presented here covers the specular (coherent) and diffuse (noncoherent) components of multipath. The test data were collected for conditions that strongly favor diffuse multipath.

Multipath can degrade radio frequency (RF) transmission by adding unwanted reflected signals to the desired direct-path signal. The unwanted signals are delayed and will consequently have a different phase than the direct-path signal. Depending on the wavelength, geometry, and surface conditions, the total multipath signal can have an amplitude approaching that of the direct-path signal. Moreover, multipath can appear to come from a specular reflection point, from a diffuse glistening surface, or partly from both. For a stationary transmitter-receiver-reflecting surface geometry, the specular reflection will have a constant phase difference with respect to the direct-path signal. The diffuse reflection consists of a collection of signals of varying amplitudes and phases. The combined multipath returns can therefore add constructively or destructively with the direct-path signal to produce a stronger or weaker (or even vanishing) total received signal. When one or both of the platforms move, the received signal will fade in and out. This fading can affect RF communications and radar target detection/tracking.

MULTIPATH MODEL

For air-to-air communications, Figure 1 shows a direct path between the transmitter and the receiver and several other paths between the transmitter and the receiver that involve scattering of RF signals off the earth's surface.[1] The propagation paths involving scattering are longer than the direct path. The path from the transmitter to the specular point (point S in the figure) and then from the specular point to the receiver defines the minimum multipath distance. However, scattering can also occur from points on either side of the specular point (i.e., those points labeled D in the figure), and these multiple paths have a longer total path length.

Specular and Diffuse Multipath

Smooth, mirror-like surfaces produce specular multipath. Although the specular multipath appears to come from a single point, it actually involves coherent integration over a wide portion of the surface. Rough surfaces produce diffuse multipath. In this case, the reflected RF signals over the surface add noncoherently and typically appear weaker than specular multipath. Diffuse multipath appears to come from a sizable region, known as a glistening surface, and it is spread in path delay (Beckmann and Spizzichino 1987; Barton 2005, 279–290). While the peak amplitude of the diffuse multipath can sometimes be relatively weak, the total strength of the diffuse multipath can become signifcant after noncoherently combining the energy coming from a large glistening surface.

In 1953, Ament developed a formula that predicts the specular reflection coeffcient, ρ_s (Ament 1953, 142–146). This formula was subsequently modified in 1984 by Miller (Miller, Brown, and Vegh 1984, 114–116) and takes the following form:

$$Ps = 2\left(\frac{2\pi\sigma_h \sin(\psi)}{\lambda}\right)^2 \tag{1}$$

$$\rho_s = \exp\left[-Ps\right] I_0\left(Ps\right), \tag{2}$$

where σ_h is the root mean square surface height variation, ψ is the grazing angle, λ is the radar's wavelength, and $I_0(\,)$ represents the modified Bessel function of the first kind.

System Response for Specular Multipath

The following equation expresses the strength of the specular return relative to the strength of the direct-path return as a function of four factors (ρ_s, $\sqrt{G_{ant}}$, Γ_p, and ρ_{veg}):

$$\frac{\text{Specular voltage}}{\text{Direct path voltage}} = \rho_s \sqrt{G_{ant}} |\Gamma_p| \rho_{veg}, \tag{3}$$

where ρ_s comes from Eq. (2), $\sqrt{G_{ant}}$ is the ratio of antenna gains between the specular and the direct paths, Γ_p is the Fresnel reflection coefficient,[2] and ρ_{veg}

[1] Due to reciprocity, the locations of the transmitter and receiver can be interchanged without affecting the theory.

[2] The Fresnel reflection coefficient is a complex value that is a function of the surface conductivity and dielectric constant, the wavelength, the grazing angle, and the polarization. The subscript p denotes the polarization.

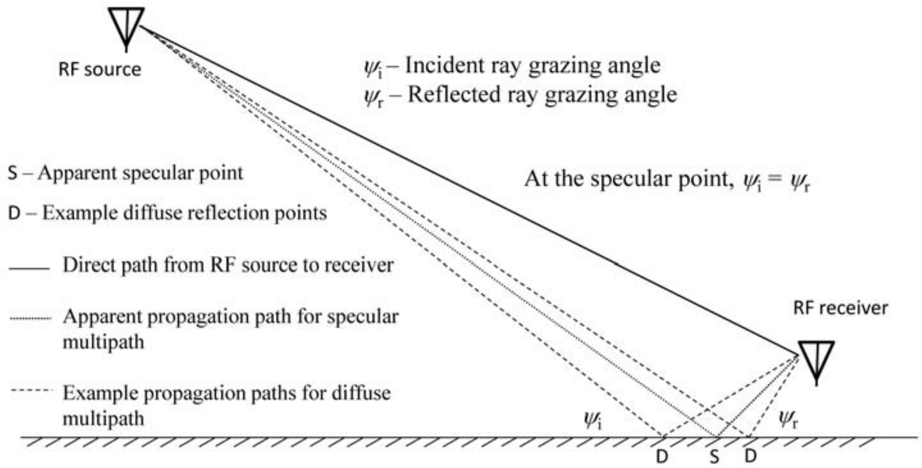

Figure 1. Multipath Geometry

represents a vegetation absorption factor. The system impulse response consists of a unit impulse at the time of arrival of the direct path pulse and a second pulse with a magnitude given by Eq. (3) delayed according to the following formula:

$$\text{Specular range delay} = R_1 + R_2 - R, \quad (4)$$

where R_1 is the distance from the transmitter to the specular point S in Figure 1, R_2 is the distance from the specular point to the receiver, and R is the direct-path distance between the transmitter and the receiver.

Glistening Surface and Diffuse Multipath

A rough surface produces scattering, but the surface roughness makes the phase relationships among the reflections across the surface unpredictable (or at least infeasible to address in anything other than a statistical sense). Barton extended the rough surface formulation of Beckmann and Spizzichino, and this extension provided the basis for formulating a single equation that describes the diffuse multipath return from an arbitrary small patch of area dA lying somewhere on the glistening surface. The last term in Eq. (5) differs from the one provided by Barton to incorporate a more rigorously derived representation of the surface shadowing that can occur at low grazing angles. This shadowing reduces the effective area for accumulating multipath diffuse energy. The resulting equation becomes

$$\frac{\text{Diffuse voltage from } dA}{\text{Direct path voltage}} = \sqrt{\frac{1}{4\pi}\left(\frac{R}{R_1 R_2}\right)^2 \frac{1}{\beta_0^2} \exp\left(-\frac{\beta^2}{\beta_0^2}\right) dA} \cdot |\Gamma_v| \cdot \rho_{veg} \cdot \sqrt{G_{ant}} \cdot \rho_{roughness} \sqrt{S_f}, \quad (5)$$

where:

$\frac{1}{4\pi}\left(\frac{R}{R_1 R_2}\right)^2$ is the one-way spreading loss;

$\frac{1}{\beta_0^2} \exp\left(-\frac{\beta^2}{\beta_0^2}\right)$ is the expected bistatic radar cross section per unit area (σ_h) of the diffuse patch defined by dA, where β_0 is the mean square value of the surface slope over the region of interest and β is the angle between the bisector of the R_1 and R_2 rays and the local vertical;

$\rho_{roughness}$ is the roughness factor (potential maximum diffuse return multiplier); and

$\sqrt{S_f}$ is the shadowing factor (probability that dA is actually seen by both the transmitter and receiver) based on previous research (Smith 1967, 668–671).

The antenna factor term in Eq. (5) is different from the specular antenna factor in that it varies over the glistening surface, as do most of the other terms in this equation.

Impulse Response Curve for Diffuse Multipath

Figure 2 shows an example of a one-way impulse response curve (IRC) for the combination of the direct path, the total (specular and diffuse) multipath, and the diffuse-only multipath. The first portion of the diffuse-return IRC combines the energies associated with those portions of the glistening surface that have a path delay within one radar range-resolution bin of the specular path delay. This example assumes that the specular energy is about 25% of the diffuse energy occurring in the same range bin. Additional portions of the glistening surface have longer path delays, and they produce a one-way diffuse IRC that results in a series of diminishing response values. The figure shows only a slight addition to the diffuse multipath due to the addition of the specular component.

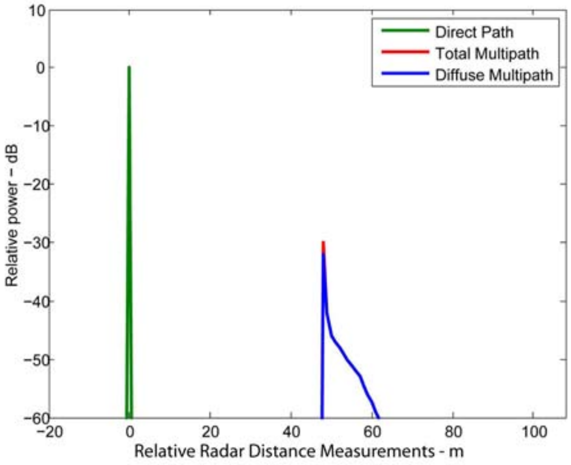

Figure 2. Example IRC

VALIDATION TESTING

The original multipath formulations that underlie the methodology did not explicitly consider their applicability to wide-bandwidth systems. Therefore, this effort addresses the foregoing theoretical formulations in the context of wideband RF systems. For this validation effort, we chose to use a wideband instrumentation radar observing a point scatterer (i.e., a calibration sphere), with a relatively rough surface between the radar and the point scatterer, and then directly observing the one-way multipath IRC.

Atlantic Test Range Experimental Configuration

The Atlantic Test Range experiments used two nominally identical high-gain X-band radar antennas sitting near the coastline of the Chesapeake Bay and a tethered sphere a few miles off shore. One of the antennas tracked the tethered sphere and bounced RF energy off it. The other antenna pointed downward and observed the glistening surface. The downward-looking antenna only received radar signals (i.e., it did not transmit) but had its local oscillator synchronized with the upward-looking antenna so it could coherently process the received multipath returns. Figure 3 illustrates the test configuration. Because the calibration sphere appears as a point source, the experiment directly measured the one-way IRC over the sphere-surface-receiver path. The relatively short ranges and low grazing angles generate an IRC with relatively little range delay, which necessitated the use of a wide-bandwidth radar to resolve the structure of the IRC.

During the test, the winds varied between 20 and 30 kts out of the north. These winds created approximately 3.5-ft waves with a period of about 3 sec. The high-gain, approximately 10-ft diameter radar antennas, have 3-dB beamwidths of about 0.66º. The upward-looking transmitting and receiving antenna, designated X1, tracked the tethered sphere as the winds blew it around. The sphere's height varied from about 310 to 475 ft, and the range varied from about 13,900 to 14,200 ft. The downward-looking, receive-only antenna, designated X2, stepped through 21 look-down angles between 4º and 0º to scan the glistening surface. The downward-looking antenna recorded data for 30 sec at each look-down step and ran through this range of look-down angles twice. The test conditions produced $\sigma_h \approx 27$ cm and $\beta_0 \approx 0.055$ radians.

Data-Analysis Procedures

The test conditions suggest that the diffuse multipath should totally dominate the specular multipath.[3] However, we wanted to validate this theoretical prediction by analyzing the data in such a way that any specular multipath significantly above the predicted value would become readily apparent. Also, the diffuse multipath model assumes a statistically random Gaussian surface. During the surface's approximately 3-sec wave period, the diffuse glistening surface should appear random, in accordance with the Gaussian assumption inherent in the diffuse multipath formulation. Therefore, we needed to use relatively long coherent processing intervals, which therefore meant that we had to perform motion compensation to remove the effects of the winds moving the tethered sphere during the data measurement intervals.

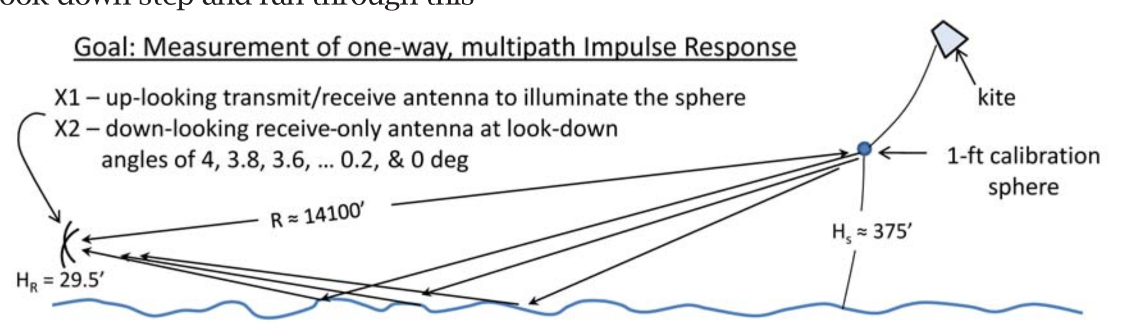

Figure 3. Atlantic Test Range Test Configuration

[3] With $\rho_S = 0.1787$, the specular power, which is related to the square of this value, becomes about 3% of the diffuse power.

RESULTS

Figure 4 shows the initial comparison of the measured and predicted IRCs after convolving the predicted multipath IRC with the inherent IRC of the measurement radar. The solid line indicates the predicted IRC, and the dashed line represents the measured IRC. While these results generally look good for positive values of relative range, the figure shows significant energy in the negative-axis portions of the measured data. This early arriving energy seemed to violate the basic principle of the speed-of-light limit for RF propagation. However, upon closer investigation, we discovered that the apparent discrepancy was most likely caused by some return energy diffracting off the edges of the Cassegrain antenna's subreflector. Figure 5 illustrates this "short-circuit" path. After accounting for this effect and combining all of the measurement data, IDA obtained the result shown in Figure 6, thereby demonstrating that the basic multipath formulations appear correct even when extended to wideband applications.

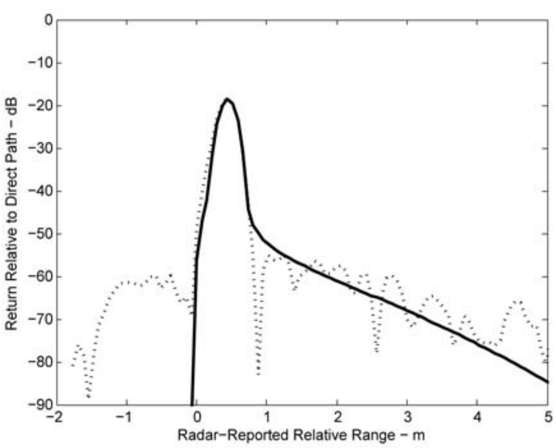

Figure 4. Initial Impulse Response Result

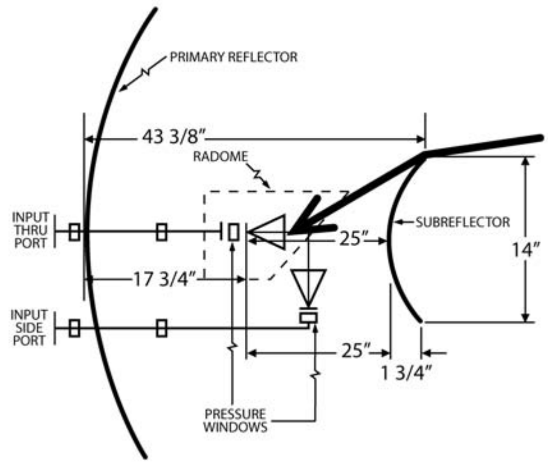

Figure 5. Antenna Diffraction Path

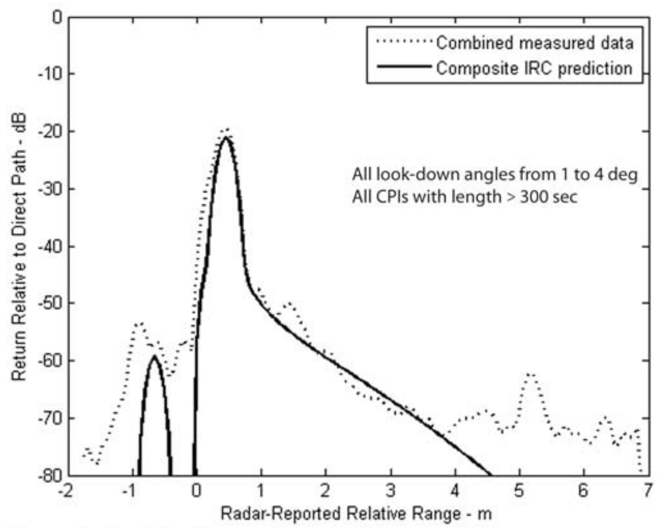

Figure 6. Combined Theoretical and Observed IRCs

Dr. Haspert holds a doctorate in electrical engineering from the University of Maryland. Mr. Tuley hold a master's degree in electrical engineering from The Georgia Institute of Technology.

The full article was published in the journal *IEEE Transactions on Aerospace and Electronic Systems*.

AN APPROACH FOR EVALUATING MULTIPATH EFFECTS

http://ieeexplore.ieee.org/stamp/stamp.jsp?tp=&arnumber=5937259

REFERENCES

Ament, W. S. 1953. "Toward a Theory of Reflection by a Rough Surface." *Proceedings of the IRE* 41 (1) (January): 142–146.

Barton, David K. 2005. *Radar System Analysis and Modeling*. Norwood, MA: Artech House.

Beckmann, Petr, and Andre Spizzichino. 1987. *The Scattering of Electromagnetic Waves from Rough Surfaces*. Norwood, MA: Artech House.

Miller, A. R., R. M. Brown, and E. Vegh. 1984. "New Derivation for the Rough-Surface Reflection Coefficient and for the Distribution of Sea-Wave Elevations." *IEE Proceedings H* 131 (2) (April): 114–116.

Smith, B. 1967. "Geometrical Shadowing of a Random Rough Surface." *IEEE Transactions on Antennas and Propagation* 15 (5) (September): 668–671.

Past Issues

Security in Africa

- Trends in Africa Provide Reasons for Optimism
- China's Soft Power Strategy in Africa
- Sudan on a Precipice
- A New Threat: Radicalized Somali-American Youth
- Chinese Arms Sales to Africa
- Outsourcing Imagination: The Potential of Informal Engagement Networks in Africa
- Defense Environmental Cooperation with South Africa

Challenges in Cyberspace

- Cyberspace – The Fifth and Dominant Operational Domain
- Transitioning to Secure Web-Based Standards and Protocols
- Information Assurance Assessments for Fielded Systems During Combatant Command Exercises
- Supplier-Supply Chain Risk Management
- Internet-Derived Targeting: Trends and Technology Forecasting
- Training and Educating the DoD Cybersecurity Workforce

Today's Security Challenges, Part II

- A Framework for Irregular Warfare Capabilities
- Bridging the Interagency Gap for Stability Operations
- Developing an Adaptability Training Strategy
- Force Sizing for Stability Operations
- Planning Forces for Steady State Foreign Internal Defense and Counterinsurgency
- Test and Evaluation for Rapid-Fielding Programs
- Understanding Security Threats in East Africa

Today's Security Challenges, Part I

- Supporting Warfighting Commands
- Detecting Improvised Explosive Devices
- Building Partner Capacity
- Combating the Trans-South Atlantic Drug Trade
- Countering Transnational Criminal Insurgents
- Using Economic and Financial Leverage
- Understanding the Conflict in Sudan

Resource Analyses

- Evaluating the Costs and Benefits of Competition for Joint Strike Fighter Engines
- Analysis and Forecasts of TRICARE Costs
- Cost Savings from the Post-Cold War Consolidation of the Defense Industrial Base: A Case Study of the Shipyards
- The Effects of Reserve Component Mobilization on Employers
- Does DoD Profit Policy Sufficiently Motivate Defense Contractors?
- Auctions in Military Compensation

Focusing on the Asia-Pacific Region

- Making American Security Partners Better Resource Managers
- Collaborating with Singapore to Better Understand the U.S. and Asian Defense Environments
- Intellectual Outreach to the Muslim World: The Council for Asian Terrorism Research
- Inside North Korea
- Red Teaming for Terminal Fury
- Promoting Interagency Cooperation in Shaping U.S.-China Relations
- Extending Trilateral Cooperation in Dealing with Disaster
- Developing Human Capital in China – Implications for the United States
- Nanotechnology in the Pacific

Net-Centric Operations

- Joint Battle Management Command and Control Roadmap Study
- Estimating the Cost of Future C4ISR Systems of Systems
- Command Post of the Future
- Deployable Joint Command and Control System Testing and Evaluation
- Operation Iraqi Freedom Bandwidth Analysis
- Framework for Achieving Joint Command and Control Capabilities

IDA | RESEARCH NOTES

4850 Mark Center Drive • Alexandria, VA 22311-1882
www.ida.org